

# Analyzing gully erosion in the Lake Manyara catchment – Tanzania



Universiteit Utrecht

**Noud Egberts**

# MSc Thesis

## June 2020

Author: Noud Egberts  
Student number: 6621511  
E-mail: [n.egberts@students.uu.nl](mailto:n.egberts@students.uu.nl)

First supervisor: Dr.ir. Geert Sterk  
Second supervisor: Drs. Maarten Zeylmans van  
Emmichoven

MSc Programme: Earth Surface and Water  
Faculty of Geosciences  
Department of Physical Geography  
Utrecht University

## **Abstract**

Despite being mentioned as an important land degradation process in the Lake Manyara catchment in Tanzania, little is known about the role of gully erosion in Lake Manyara catchment. Lake Manyara is a basin with no outflow making it vulnerable to local sediment dynamics. The biodiversity is high and the national park that is located in the Lake Manyara catchment is an important source of income for the region. A combination of fieldwork and modeling with SWAT was implemented to study gully erosion in the catchment. The fieldwork measurements consisted of the inserting erosion pins in and around the gully heads and channels of two different gully systems and measuring the growth. Additionally, SWAT was used to model the surface runoff and sediment yield that is transported into one of the two studied gully systems. Further, SWAT was also implemented to study a scenario in which the agricultural land cover in the area is increased. The measured sediment mobilization ranged from 0.01 to 1.71 m<sup>3</sup> per month. In the modeled catchment an average sediment yield which ranged from 4.5 to 15.7 t/ha/yr was found. For the scenario with increased agricultural land cover, the sediment yield increased significantly. The exact amount of sediment that ends up in the lake is unknown, but the current study provides an indication of the magnitude of sediment erosion in the catchment.

# Contents

|  |           |
|--|-----------|
| <b>Abstract</b>  | <b>i</b>  |
| <b>1 Introduction</b>                                    | <b>1</b>  |
| 1.1 Study area . . . . .                                 | 4         |
| <b>2 Materials and methods</b>                           | <b>6</b>  |
| 2.1 Remote Sensing (RS) analysis . . . . .               | 6         |
| 2.2 Fieldwork overview . . . . .                         | 6         |
| 2.3 Field measurements . . . . .                         | 7         |
| 2.4 Data analysis . . . . .                              | 8         |
| 2.5 Modeling . . . . .                                   | 8         |
| 2.5.1 Land phase . . . . .                               | 9         |
| 2.5.2 Water routing phase . . . . .                      | 12        |
| 2.5.3 Model application and scenarios . . . . .          | 13        |
| 2.5.4 Input data . . . . .                               | 13        |
| 2.5.5 Model Evaluation . . . . .                         | 14        |
| <b>3 Results</b>   | <b>14</b> |
| 3.1 Gully systems in the study area . . . . .            | 15        |
| 3.2 RS analysis . . . . .                                | 16        |
| 3.3 Precipitation measurements . . . . .                 | 17        |
| 3.4 Gully head monitoring . . . . .                      | 18        |
| 3.5 Channel bed erosion measurements . . . . .           | 21        |
| 3.6 Relation precipitation and gully erosion . . . . .   | 22        |
| 3.7 Mobilized sediment in the gully systems . . . . .    | 23        |
| 3.8 Vegetation . . . . .                                 | 25        |
| 3.9 Modeling of Land Use and Land Cover change . . . . . | 27        |
| 3.9.1 Current situation . . . . .                        | 29        |
| 3.9.2 Precipitation, erosion, and runoff . . . . .       | 31        |
| 3.9.3 Increasing agricultural land cover . . . . .       | 31        |
| 3.10 Validation . . . . .                                | 32        |
| <b>4 Discussion and Conclusion</b>                       | <b>33</b> |
| <b>5 References</b>                                      | <b>36</b> |
| <b>6 Appendix</b>  | <b>43</b> |
| 6.1 Appendix A . . . . .                                 | 43        |
| 6.2 Appendix B . . . . .                                 | 44        |

# 1 Introduction

Healthy soils are essential to life on earth. Deep and fertile soils are the foundation of agriculture and are thus a fundamental resource for mankind (Borrelli et al., 2013; Montanarella et al., 2016). Soils play a crucial part in the world's ecosystems and are essential for delivering many ecosystem services such as food, drinking water, climate regulation, and many others (Borrelli et al., 2013).

There are however many regions in the world in which the quality of the soils is declining. One of these regions is East Africa (Borrelli et al., 2013; Wynants et al., 2019). Due to exponential population growth of 24 million in the 1950s to 173 million in 2017 and subsequently land cover and land use changes, the pressure on the natural environment has been increasing (Wynants et al., 2019). A recent study by Maitima et al. (2019) found that land use and land cover in this region has mainly changed from natural area into agroecosystems such as farmlands, and grazing lands but also into urban area (Maitima et al., 2019). These changes are associated with land degradation and the main process causing land degradation in this area is soil erosion (Wynants et al., 2019).

The East African Rift System (EARS) contains some of the highest soil erosion rates in the world in part because of its steep elevation gradients and the semi-arid climate, but also because of the land use and land cover changes (Blake et al., 2018). Agriculture is the main cause of soil erosion in this region (Wynants et al., 2019). Within the EARS many pastoralists herd their livestock on the savannas (Homewood et al., 2012). After colonial times new legal systems were implemented in this region which lead to the privatization of many formerly communally owned lands (Homewood et al., 2012; Wynants et al., 2019). The new centralized agricultural system brought about many changes. The livestock numbers more than doubled over the past 50 years causing overgrazing and soil trampling (Wynants et al., 2018). Furthermore, the privatization of many formerly communally owned lands decreased their mobility and pushed farmers to lands less suitable for agriculture. Finally, the exploitation of woodlands and forests as a source of fuel in this area was observed (Wynants et al., 2019). These changes all increased the susceptibility of the soils in this region to erosion.

The Monduli district in the Arusha region located in Northern Tanzania is typical for the types of land degradation that are found in the EARS (Kiunsi & Meadows, 2006). This area is home to approximately 158.000 people, most of which are Maasai (Kiunsi & Meadows, 2006; National Bureau of Statistics, 2013). The Masaai are an ethnic group of agro-pastoralists who occupy an area of 150.000 km<sup>2</sup>, which stretches over rangelands in both northern Tanzania and southern Kenya (Homewood et al., 2009). Besides being home to this unique ethnic group the area is also well known for its large number of wildlife species (Homewood et al., 2012). A recent study by Wynants et al. (2018) concluded that there was a net change in land cover from natural and semi-natural towards agricultural use in this area, which contributes to an in-

creasing soil erosion risk.

The Monduli district partly contains the Lake Manyara catchment which will be the focus of the current study. Lake Manyara is a basin that has no outflow making it vulnerable to local sediment dynamics. The catchment also contains a national park on the western side which is important for both the conservation of wildlife in the area and protection of natural areas, but also for the local and regional economy due to income from the tourism sector (Wynants et al., 2018). Initially, it was thought that the lake was disappearing, but studies suggest that this is not the case. The shrinkage and growth of the lake surface show a cyclic nature and the intervals between the large and smaller lake extent seem to be getting longer (Van Mens, 2016). Another problem that has been put forward is increased sedimentation rates in the lake caused by a complex interaction of increased upstream sediment mobilization from natural precipitation dynamics and land-use changes (Wynants et al., 2020; Blake et al., 2018). The increased sediment input can degrade the water quality, cause diminishment of the lake size, and thus decrease the overall health of the lake (Xu et al., 2017). Nevertheless, the effect, magnitude, and responsible processes of soil erosion in the Lake Manyara catchment remain unknown since very few studies have focused on this. It has been reported that one specific type of soil erosion has become more severe over the past few decades, namely gully erosion (Blake et al., 2018). This type of soil erosion can dramatically increase the sediment concentration in river networks (Maerker et al., 2015). Blake et al. (2018) state that gully erosion in the Lake Manyara catchment is a major source of sediment. They mention in their study that gully networks efficiently connect sheet and rill erosion and enhance surface runoff flow to downstream channel networks, and thus increasing the hydrological connectivity.

Gully erosion is the development of U-, V- or trapezoidal-shaped channels in the landscape (Bashir et al., 2019; Kirkby & Bracken, 2009). Figure 1 shows the stages of development of a gully. Gullies thus result from concentrated surface runoff and remove soil and parent material (Kirkby & Bracken, 2009). A distinction can be made between permanent, also called classical, and ephemeral gullies. The former refers to gullies which are too large to be crossed with farming equipment and cannot be obliterated by normal tillage operations (Kirkby & Bracken, 2009). Ephemeral gullies are defined as gullies which are, just as classical gullies, formed by concentrated overland flow but can still be filled by normal tillage operation (Hoogenboom, 2013). Furthermore, a distinction can be made based on the activity of the gully. Active gullies are far from equilibrium and morphological processes are active in changing the shape and size of the gully. Active gullies are incising, and rapid mass-movements occur frequently (Sidorchuk, 2006). Stable channels usually have a long and smooth profile and vegetation can grow on the walls increasing the stability of the gully (Capra, 2013; Sidorchuk, 2006). For the current study, the focus will be on active gully systems.

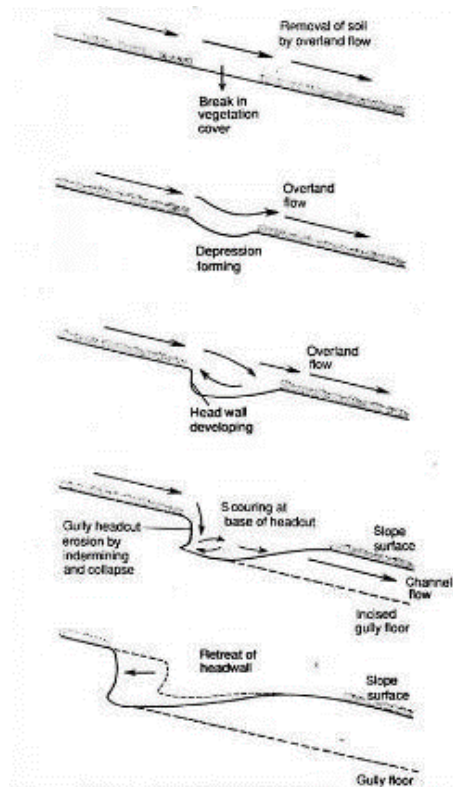


Figure 1: Stages of development of a gully. Source: Leopold et al. (1964).

Several ways exist in which gullies can contribute to sediment production in a catchment. The first process causing sediment production is gully head cut retreat also called headwall erosion. The process of gully head cut retreat is the same process that occurs in waterfalls but on a smaller scale. The energy of the runoff that flows through the surface depression actively removes material and transports it down into the gully channel causing a plunge pool at the gully head (Flores-Cervantes, Istanbuluoglu & Bras, 2006). Turbulence in the plunge pool is an important mechanism inducing undercutting of the headwall which potentially leads to further instability of the headwall and thus increasing the removal of material (Flores-Cervantes, Istanbuluoglu & Bras, 2006). Another similar process is headwall and sidewall collapse or failure because of gravitational forces that work on the weakened head or sidewall. These processes can account for 50% of the sediment production in gullies (Martinez-Casasnovas et al., 2004). When the material of the walls is saturated it becomes heavier and more unstable if tension cracks are also present, the throughflow of water in the walls is enhanced further increasing the instability and eventually leading to failure of the side walls or gully headwall (Martinez-Casasnovas et al., 2003). Flowing water inside the channels also

causes instability by removing soil at the base of the walls causing bank scour in the gully channels (Martinez-Casasnovas et al., 2003). Furthermore, other factors enhancing instability exist such as the slope of the walls and various soil characteristics (Martinez-Casasnovas et al., 2003). There is not one value for the critical slope since it is interrelated with many other variables. Channel bed erosion is another sediment source, the amount of which is strongly dependent on the energy of the flowing water but also on soil characteristics (Wu et al., 2008). Finally, an indirect cause of sediment production results from the fact that gully systems serve as conveyance routes in which sediment that is mobilized in the catchment by other processes such as the previously discussed sheet and rill erosion is efficiently transported downstream (Blake et al., 2008).

Even though different studies mention gully erosion to play a part in the sediment contribution little is known about the mechanisms behind the gully formation, expansion and the amounts of sediment that are produced (African Wildlife Foundation, 2003; Maerker et al., 2015; Wynants et al., 2018). Gaining knowledge about gully erosion is essential in understanding the dynamics and interactions between soils and their surrounding environment. The current study aimed to quantify the sediment production as a result of gully erosion in the Lake Manyara catchment. Moreover, the study evaluated which processes are actively producing sediment in the gully system since little is known about this topic. The following Specific objectives were defined for the study:

1. Determining the growth rate and other characteristics of the gullies in the Lake Manyara Catchment.
2. Modeling the sediment yield and surface runoff in a selected sub-catchment.
3. Model the effects of land-use change on surface runoff and sediment yield in selected gully systems.

## 1.1 Study area

The study area (fig. 2a & b) is characterized by tectonic activity and volcanism which formed the EARS. The topography that is the result of this tectonic movement still shapes the hydro- and morphological processes in this region (Deus et al., 2013). A long stretching escarpment can be found on the western side of the catchment, this area contains steep elevation gradients while the eastern side contains gentle slopes, beside a few secluded volcanic cones (Deus & Gloaguen, 2013). Lake Mayara is the southernmost lake in the eastern arm of EARS and it is characterized by shallow water depth and saline waters (Deus & Gloaguen, 2013). The lake is dynamic, and its maximum surface area varies between 410 and 480 km<sup>2</sup>. Studies have shown that in the past the lake has also dried up completely (Deus et al., 2013). The region has been through many social changes and related land use and land cover changes. Wynants et al. (2018) concluded that land cover types in this area are highly dynamic and

that there is a net conversion of different types of natural land cover to agricultural land cover. The accuracy of these results has however been questioned by the study of Verhoeve (2019), who could not identify clear land cover changes over the last 40 years from available Landsat imagery.

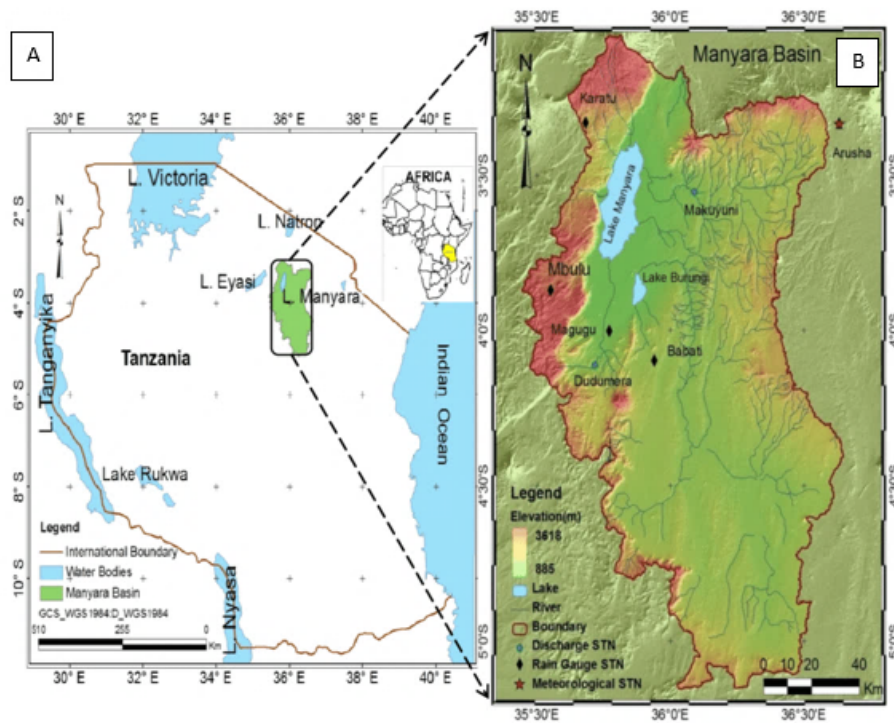


Figure 2: A is the location of the Lake Manyara Catchment in Tanzania. B is the catchment area of Lake Manyara in more detail. Source: Deus et al. (2013).

The two dominant soil types which can be found in the catchment area are luvisols, accounting for 23%, and andosols, which are found in 16% of the study area (Van Mens, 2016). The gullies that were studied in the field are located on the eastern side of the lake between the villages of Mto Wa Mbu and Makuyuni, and the second study area is located on the western side of the lake in the Lake Manyara National Park. Research by Wynants (2018) on the sediment contribution of different sub-catchments to Lake Manyara identified the Makayuni sub-catchment East of the lake as being the largest contributor of sediment to the lake. It is also this sub-catchment where the first study area is located. With the help of radionuclide tracing, it was found that 59.3% of the sediment that was sampled from the top layers in Lake Manyara originates from the Makuyuni sub-catchment (Wynants, 2018), which will be discussed in more detail in the next section.

The precipitation in the area is variable. The higher plains receive up to 1200

mm per year, while the lower-lying planes receive just 700 mm per year (Bachofer et al., 2014; Deus & Gloaguen, 2013). The annual cycle contains two dry and two wet seasons. The first wet season, which is relatively short, occurs from November to December. This is followed by a short dry season from January to February. Then there is the second longer wet season that occurs from March to May. Finally, there is a long dry period stretching from June to October (Deus & Gloaguen, 2013). The average temperature is in a range between 15 and 25°C (Deus & Gloaguen, 2013).

## 2 Materials and methods

### 2.1 Remote Sensing (RS) analysis

Images that are available on *Google Earth Pro* were used to map existing gullies and to identify potential fieldwork sites. The first step was visual identification of the gullies, followed by the construction of polygons around the identified gully heads. Comparing the gully extent with its previous extent indicates the growth rates, although it should be mentioned that on the satellite images it can be hard to see the difference between the gully head and the eroded or bare soil that surrounds it, this could cause overestimation of the actual size. Nevertheless, this technique can yield valuable information on gully growth rates. Two gully systems have been identified as potential fieldwork sites; they will be discussed in more depth in the next section.

### 2.2 Fieldwork overview

The fieldwork areas were selected based on their accessibility, activity of the gullies, and connectivity to Lake Manyara. Gully system 1 (GS1) is located between the village of Mto Wa Mbu and Makuyuni. This area contains sparsely scattered vegetation mostly consisting of *V. Drepanolobium* trees. A sandstone layer is present at different depths. The area is used daily by Maasai who roam around with their grazing cows and/or goats. The gully system in this area is extensive and well connected to other gully systems in the area. Gully system 2 (GS2) is in the Lake Manyara National Park. This gully system is smaller than GS1 (Table 1). To the north of the main channel, there is a road. One major difference between GS1 and GS2 is that GS2 is in the national park in which human interaction with nature is minimized. Nevertheless, there are roads, bridges, and drainage channels along the main roads. Grazing by large herds of domesticated animals, however, does not occur inside the park. Fieldwork was performed between 28/11/2019 and 27/1/2020. Measurements consisted of gully head monitoring, dimension measuring, and soil sampling. The methods will be discussed in more detail in the next section.

Table 1. Overview of the main characteristics of the two studied gully systems (GS1 and GS2) in the Lake Manyara catchment, North Tanzania.

| Characteristics                       |            |      |           |      |  |  |                   |                   |
|---------------------------------------|------------|------|-----------|------|--|--|-------------------|-------------------|
| Gully name                            | dimensions |      |           |      | Vegetation   | Natural disturbance  | Soil              | Shape             |
|                                       | Width (m)  |      | Depth (m) |      |  |  |                   |                   |
|                                       | max        | min  | max       | min  |  |  |                   |                   |
| GS1<br>3°29'18.42"S,<br>35°59'42.70"E | 814        | 2522 | 130       | 799  | Scattered<br>Drepanolobium, short<br>grasses. But around the<br>gully channel mostly dry<br>unvegetated soil | V.<br>Human and animal<br>interaction. Herds of<br>goats and cows<br>walking through the<br>gully channel. | Swelling<br>clays | U,<br>Trapezoidal |
| GS2<br>3°26'6.63"S,<br>35°48'28.47"E  | 410        | 530  | 0,75      | 0,80 | Short to medium-high<br>grasses. Also different<br>types of Drepanolobium.                                   | Animal interaction.<br>Mostly elephant<br>trampling the gully<br>sidewalls.                                | Swelling<br>clays | U,<br>Trapezoidal |

### 2.3 Field measurements

According to Hoogenboom (2013) if one of the following features is observed a gully is said to be active:

1. Undercut or plunge pool causing a cave-in
2. A vertical or nearly vertical wall
3. No vegetation on the gully wall
4. Tension cracks
5. Sidewall collapse and sediment on the gully floor

Around active gully heads - based on the criteria of Hoogenboom (2013) - and inside gully channels the head cut retreat and channel bed erosion were monitored with the help of erosion pins. These are metal pins with a diameter of 4mm and a length of 25cm that were inserted around the headwall and in the channel bed (Hessel & Van Asch, 2003). In total 33 erosion pins were placed around gully heads and 11 pins were placed inside different channels in both GS1 and GS2. After each precipitation event, the length of the erosion pins was measured within the channel bed. The gully head measurements were different and consisted of measuring the distance between the erosion pin and the gully headwall. This yields information on the growth rate of the gully heads and the erosional and depositional dynamics inside the gully channel.

On different occasions, measurement equipment was removed by local people in GS1. This problem was tried to solve by exchanging the metal erosion pins with wooden sticks for some of the study sites. The erosion pin measurements are most valuable when combined with accurate precipitation data, but since

onsite precipitation measurements in GS1 and GS2 were not possible, the precipitation data were collected from the nearest rain gauge locations. For GS1 precipitation data were collected in the village of Mto Wa Mbu, which is 18km from GS1, and for GS2 the precipitation data were collected from a rain gauge at the gate of the National Park, located 9km from GS2.

With the help of detailed cross-sections, morphology-change, and growth processes were studied. These cross-sections were measured with a measuring tape. Cross-sections 1 to 3 were measured with high detail, but due to limitations in equipment and the time-consuming process, the other cross-sections were measured in a more simplified manner. The simplified cross-sections used an inclinometer to measure the sidewall slopes and the length of the sidewalls was measured with a measuring tape. For the channel bed, the measuring interval was much larger causing only major profile features to appear in the cross-section diagrams. The cross-sections were used to analyze the strengthening effect of vegetation on the sidewalls (Feng et al., 2017). For all sidewalls, the slope was determined by computing the tangent and subsequently analyzed if there is a difference between slope steepness with and without vegetation cover.

## 2.4 Data analysis

To determine the growth rates of the gully heads an average growth rate for each gully was calculated by averaging the measurements over the total period. This was done because not all gully heads had an equal amount of erosion pins around them and using the sum of all erosion pins would thus cause a bias. The same was done for other situations where using the totals would cause bias because of the unequal number of erosion pins or other measurements. Various statistical techniques have been used in the current study. Both correlation of the erosion pin measurements for each gully head and the measured precipitation, and the correlation between rainfall and channel bed erosion were analyzed with the help of the *Pearson correlation coefficient*  $r$ . Another technique that was used is a *t*-test performed at  $p < 0.05$  to analyze whether a difference existed in the growth rates in GS1 and GS2. Moreover, the effects of vegetation on the sidewall slopes was also studied with a *t*-test. For the statistical analysis, not all erosion pin data could be used due to difficulties during the fieldwork such as the removal of research equipment and disappearance due to heavy precipitation. The data of 9 channel bed erosion pins and 13 gully head erosion pins have been used in the actual data analysis. All statistical analyses were carried out using Microsoft Excel.

## 2.5 Modeling

Modeling was applied to quantify the surface runoff and sediment detachment and transport within the Lake Manyara catchment. Moreover, modeling can provide valuable insights into the effects of future land-use changes on surface runoff and sediment yield. The Soil Water Assessment Tool (SWAT) was used

for this purpose. The model was run on ArcGIS 10.5.1 as an extension (ArcSWAT). SWAT is a hydrologic model that can greatly aid the understanding of the hydrological processes that are related to gully erosion and formation (Neitsch et al., 2011). The model has been widely used in studies on soil erosion (Qiu et al., 2012). SWAT allows the integration of climatic, hydrological, and biological data such as vegetation characteristics. It is well known that vegetation and land use have a profound effect on erosion susceptibility of the soil (Zhang et al., 2015).

The model divides the watershed into sub-basins or sub-watersheds, which are related spatially, and then further divided into so-called hydrological response units (HRUs) (Githui et al., 2009). These HRUs are the smallest spatial units in the model and contain similar land use, land covers, and soil, and add to the complexity and accuracy of the model (Githui et al., 2009). The driving force behind everything that happens in SWAT is the water balance. For SWAT to determine the movement of sediment, nutrients, and pesticides the hydrologic cycle is modeled (Neitsch et al., 2011). The hydrologic cycle is divided into land and the water routing phase (Neitsch et al., 2011). In the land phase, the model calculates the amount of runoff, sediment, nutrient, and pesticide loadings that flows to the main channel of each sub-catchment (Van Mens, 2016). The water routing phase determines the movement of the sediment and water from the channels in each sub-catchment towards the outlet of the watershed (Githui et al., 2009; Van Mens, 2016).

The hydrologic cycle is based on the water balance equation that is at the base of SWAT (Neitsch et al., 2011):

$$SW_t = SW_0 + \sum_{i=1}^t (R_{day} - Q_{surf} - E_{\alpha} - \omega_{seep} - Q_{gw}) \quad (1)$$

In this equation  $SW_t$  is the water content of the soil in mm,  $SW_0$  is the initial content of water in the soil on day 0, also in mm.  $R_{day}$  is the precipitation on day  $i$  in mm, and  $Q_{surf}$  refers to the surface runoff on day  $i$  in mm,  $E_{\alpha}$  is the evaporation amount on day  $i$  in mm, and  $\omega_{seep}$  is the amount of water entering the unsaturated zone in mm on day  $i$  (Neitsch et al., 2011). Finally,  $Q_{gw}$  is the amount of return flow in mm on day  $i$  (Neitsch et al., 2011).

### 2.5.1 Land phase

**Surface runoff** In the current study, the SCS curve number was used to calculate the surface runoff (Githui et al., 2009). The SCS curve number equation is:

$$Q_{surf} = \frac{(R_{day} - I_{\alpha})^2}{(R_{day} - I_{\alpha} + S)} \quad (2)$$

$Q_{surf}$  is the runoff in mm,  $R_{day}$  is the daily precipitation depth (mm),  $S$  the

retention parameter (mm),  $I_{\alpha}$  the loss through the initial abstractions (mm). The retention parameter  $S$  is calculated with the following equation:

$$S = 25.4 \left( \frac{1000}{CN} - 10 \right) \quad (3)$$

In this formula,  $CN$  is the curve number of the day, which is a function of the land use, soil water conditions, and the permeability of the soil (Neitsch et al., 2011).

The  $CN$  is directly related to  $S$  through the following equation:

$$CN = \frac{25400}{(S + 254)} \quad (4)$$

The SCS curve number is a function of the permeability of the soil, the soil water conditions, and land use (Neitsch et al., 2011). Table 2 shows an example of the specific curve numbers for various land covers and soil groups. A distinction is made between four soil groups (A-D) where A has the lowest runoff potential and D the largest runoff potential (Neitsch et al., 2011).

Table 2. SCS curve numbers for different land cover types.

| Cover type   | Hydrologic condition | Hydrologic soil group |    |    |    |
|--|----------------------|-----------------------|----|----|----|
|  |                      | A                     | B  | C  | D  |
| Pasture, grassland, or range – continuous forage for grazing | Poor                 | 68                    | 79 | 86 | 89 |
|  | Fair                 | 49                    | 69 | 79 | 84 |
|  | Good                 | 39                    | 61 | 74 | 80 |
| Brush- brush-weed-grass mixture with brush the major element | Poor                 | 48                    | 67 | 77 | 85 |
|  | Fair                 | 35                    | 56 | 70 | 77 |
|  | Good                 | 30                    | 48 | 65 | 73 |
| Row crops (contoured)  | Poor                 | 70                    | 79 | 84 | 88 |
|  | good                 | 65                    | 75 | 82 | 86 |

**Evapotranspiration** Within the hydrological cycle, evaporation is the primary process that removes water from a watershed, approximately 62% of all precipitation is removed by this process (Neitsch et al., 2011). The evapotranspiration is calculated using the potential evapotranspiration (PET) (Neitsch et al., 2011; Van Mens, 2016). SWAT gives three possible methods for calculating PET all having their limitations and strengths. In the current study, the Penman-Monteith equation was used, since all required inputs (solar radiation, air temperature, relative humidity, and wind speed) were available. The Penman-Monteith equation is (Neitsch et al., 2011):

$$\lambda E = \frac{\Delta * (H_{net} - G) + \rho_{air} * c_p * [e_z^0 - e_z] / r_\alpha}{\Delta + \gamma * (1 + r_c / r_a)} \quad (5)$$

$\lambda E$  is the density of the latent heat flux ( $\text{MJ m}^{-2} \text{ m}^{-1}$ ),  $E$  is the depth rate of the evaporation in mm per day,  $\Delta$  is the slope of the saturation vapor pressure-temperature curve,  $de/dT$  ( $\text{kPa } ^\circ\text{C}^{-1}$ ),  $H_{net}$  is the net radiation ( $\text{MJ m}^{-2} \text{ d}^{-1}$ ),  $G$  is the density of the heat flux towards the ground ( $\text{MJ m}^{-2} \text{ d}^{-1}$ ),  $\rho_{air}$  is the density of the air ( $\text{kg m}^{-3}$ ),  $c_p$  is the specific heat at constant pressure ( $\text{MJ km}^{-1} \text{ } ^\circ\text{C}^{-1}$ ),  $e_z^0$  is the saturation vapor pressure of air at a certain height ( $z$ ) in kPa,  $e_z$  is the pressure of the water vapor at height  $z$  also in kPa,  $\gamma$  is the psychrometric constant ( $\text{kPa } ^\circ\text{C}^{-1}$ ),  $r_c$  is the plant canopy resistance ( $\text{s m}^{-1}$ ), and  $r_\alpha$  is the aerodynamic resistance ( $\text{s m}^{-1}$ ) (Neitsch et al., 2011).

The  $r_\alpha$  (aerodynamic resistance) is calculated with:

$$r_\alpha = \frac{\ln\left[\frac{z_w - d}{z_{om}}\right] \ln\left[\frac{z_p - d}{z_{ov}}\right]}{k^2 u_z} \quad (6)$$

where  $z_w$  is the height of the wind speed measurement (cm),  $z_p$  is the height of the humidity measurement (cm),  $d$  is the zero plane displacement of the wind profile (cm),  $z_{om}$  is the roughness length for momentum transfer (cm),  $z_{ov}$  is the roughness length for vapor transfer (cm),  $k$  is the von Karman constant (-), and finally  $u_z$  is the wind speed at height  $z_w$  ( $\text{m s}^{-1}$ ).

The formula for the canopy resistance is (Neitsch et al., 2011):

$$r_c = r_l / (0.5 * LAI) \quad (7)$$

$r_c$  is the canopy resistance ( $\text{s m}^{-1}$ ),  $r_l$  is the minimum effective stomatal resistance of a single leaf ( $\text{s m}^{-1}$ ), and  $LAI$  is the leaf area index of the canopy of the vegetation (Neitsch et al., 2011; Van Mens, 2016).

Finally, the  $\omega_{seep}$  is calculated with:

$$\omega_{seep} = w_{perc,ly=n} + w_{crk,btm} \quad (8)$$

Where  $w_{perc,ly=n}$  is the amount of water that percolates out of the lowest layer ( $n$ ) within the soil profile on day  $i$  (mm H2O).  $w_{crk,btm}$  is the amount of water past the lower boundary of the soil due to bypass flow on day  $i$  (mm H2O) (Neitsch et al., 2011)

**Groundwater** Unconfined aquifers cause a return flow to stream within the watershed, while deep confined aquifers involve a return flow to streams outside of the watershed (Neitsch et al., 2011; Van Mens, 2016). The water

balance of the shallow aquifer contains recharge flow entering the aquifer, the water moving into the soil zone because of a water deficit, groundwater flow, and finally the removal of water through pumping (Van Mens, 2016). The deep aquifer's water balance consists of the percolation of water from the shallow aquifer towards the deep aquifer and the amount of water that is removed from the deep aquifer by pumping (Van Mens, 2016). The  $Q_{gw}$  is however expected to be very small if not zero in the study area.

### 2.5.2 Water routing phase

The routing phase involves the routing of water and sediments through the watershed towards the outlet (Van Mens, 2016). The main channel routing is divided into four components: flood routing, nutrient routing, channel, and pesticide routing, and finally sediment routing (Neitsch et al., 2011). Water is routed through the channel or reach network using the variable storage routing method which is based on the continuity equation (Neitsch et al., 2011). The continuity equation is:

$$V_{in} - V_{out} = \Delta V_{stored} \quad (9)$$

$V_{in}$  is the volume of inflow during the time step ( $m^3 H_2O$ ),  $V_{out}$  is the volume of outflow ( $m^3 H_2O$ ),  $V_{stored}$  is the change in the stored volume ( $m^3 H_2O$ ). The formula for the average inflow rate  $q_{in,ave}$  is:

$$q_{in,ave} = \frac{q_{in,1} + q_{in,2}}{2} \quad (10)$$

$q_{in,1}$  is the inflow rate at the start of the timestep ( $m^3/s$ ),  $q_{in,2}$  is the inflow rate at the end of the timestep ( $m^3/s$ ) (Neitsch et al., 2011).

The travel  $TT$  time is calculated by dividing the water volume in the channel by the flow rate:

$$TT = \frac{V_{stored}}{q_{out}} = \frac{V_{stored,1}}{q_{out,1}} = \frac{V_{stored,2}}{q_{out,2}} \quad (11)$$

$TT$  is the travel time (s),  $V_{stored}$  is the volume that is stored ( $m^3 H_2O$ ), and  $q_{out}$  is the discharge rate ( $m^3/s$ ). The relationship between the travel time and the storage coefficient is obtained with equation:

$$q_{out,2} = SC \left( q_{in,ave} + \frac{V_{stored,1}}{\Delta t} \right) \quad (12)$$

Where  $SC$  is the storage coefficient is calculated using:

$$SC = \frac{2 * \Delta t}{2 * TT + \Delta t} \quad (13)$$

$V_{out,2}$  is then calculated as follows:

$$V_{out,2} = SC * (V_{in} + V_{stored,1}) \quad (14)$$

### 2.5.3 Model application and scenarios

SWAT was used to quantify the amounts of surface runoff and sediment that are transported towards GS1. In addition, SWAT was used to study the effects of changing land use on erosion. Two scenarios were modeled; a baseline scenario with the current situation (0.4% of agricultural land), and a scenario in which the modeled section of the watershed contains 25% of agricultural land. These scenarios are based on recent research by Wynants et al. (2018). The full catchment of GS1 with an area of 6 km<sup>2</sup> was used for the modeling.

### 2.5.4 Input data

Various sources have been used in the process of attaining the input data that is needed for SWAT. An overview of those sources can be found in table 3. The land use and land cover (LULC) map were made available by Wynants (2018), who used Landsat imagery to create the LULC map of the Lake Manyara catchment for 2016. The LULC types of the map were renamed to classes that could be used in SWAT. A DEM with a 12.5m resolution from the Advanced Land Observing Satellite Phased Array Type L-band Synthetic Aperture Radar (ALOS PALSAR) was used (ASF, 2015). 15 images have been merged into one raster image and subsequently, the image was clipped to the size of the catchment. The DEM is used by SWAT to delineate the watershed, sub-basins, and finally the HRUs. The HRU definition process also considers land cover and soil characteristics. A global-scale soil map with a spatial resolution of  $\approx 1$ km was used, which was retrieved from FAO (FAO, 1991). This soil map is based on the FAO-UNESCO legend, which makes a distinction between 106 different soil types (FAO, 1991). Finally, weather data from 1979 till 2014 was retrieved from Climate Forecast System Reanalysis (CFSR), this included daily precipitation, relative humidity, wind speed, and solar radiation (CFSR,2020).

Table 3. Overview of SWAT input data and sources.

| Data                    | Source   |
|-------------------------|--|
| Weather data            | Online database ( <i>CFSR: 2020</i> )                |
| DEM                     | Online database ( <i>ASF, 2015</i> )                 |
| Land use/land cover map | Dataset from previous study ( <i>Wynants, 2018</i> ) |
| Soil map                | Online database ( <i>FAO, 1991</i> )                 |
| Validation data         | Literature ( <i>Vanmaercke, 2014</i> )               |

### 2.5.5 Model Evaluation

It was not possible to calibrate the model because no in-situ data such as discharge or surface runoff was available to use for calibration. Therefore, the focus has been on validating the current modeling results with existing quantitative data from similar studies in this region (Karamage, 2018; Vanmaercke, 2014). The validation focused on the generated surface runoff and sediment yield. Vanmaercke (2014) reviewed 682 catchments in Africa from 84 different studies that studied sediment yield. Karamage (2018) on the other hand focused on studying the runoff in Africa. The latter study examined the relationship between runoff and precipitation at three scales: continental, river basin, and country. 25 basins and 55 countries have been analyzed. The two studies have been used to validate the results that were produced in the current study.

## 3 Results

### 3.1 Gully systems in the study area

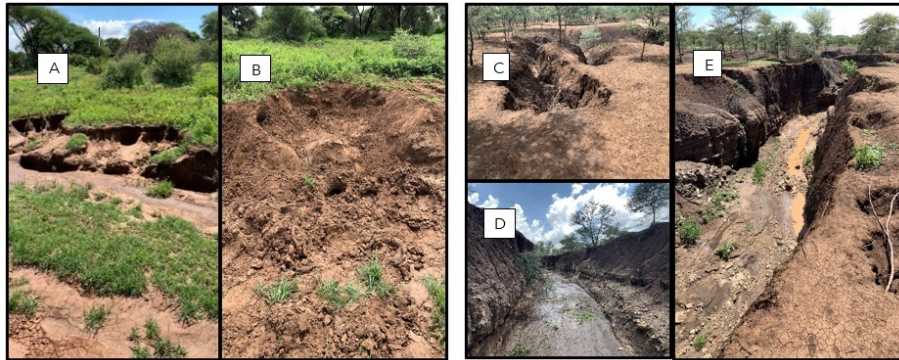


Figure 3: A and B are pictures that were taken in Lake Manyara National Park (GS2). A shows two gully heads and the main gully channel. B shows the effect of trampling of a measurements site by elephant. Picture 3C and E were taken in GS1. C shows a gully head and the bare soil which is characteristic for the area surrounding GS1. D was taken inside the main channel of GS1, and E shows the main channel from a different perspective.

During the interpretation of the data, it is important to realize the difference in the contexts of GS1 and GS2. Figure 3 contains images that show the different characteristics of both gully systems. The first major difference is in their dimensions; GS1 has sections with a depth of 7.9m and a width of 25m while GS2 has a maximum depth of 0.80m and a width of 5.30m. Another important difference that is visible in figure 3 is the vegetation. GS2 has diverse vegetation ranging from small to medium-high grasses and shrubs to different types of Acacia trees. In GS1 there is mostly bare soil with sparsely scattered Acacia trees. In addition to the natural forces that work upon the gully system in GS1, the gully system in GS2 is also being modified by elephants that walk through the gully channel and cause severe erosion. Figure 4 shows the full extent of the gully systems that were used for the fieldwork. The section of GS1 that was focused on during data collection is 809m while the section in GS2 was 349m.

### 3.2 RS analysis

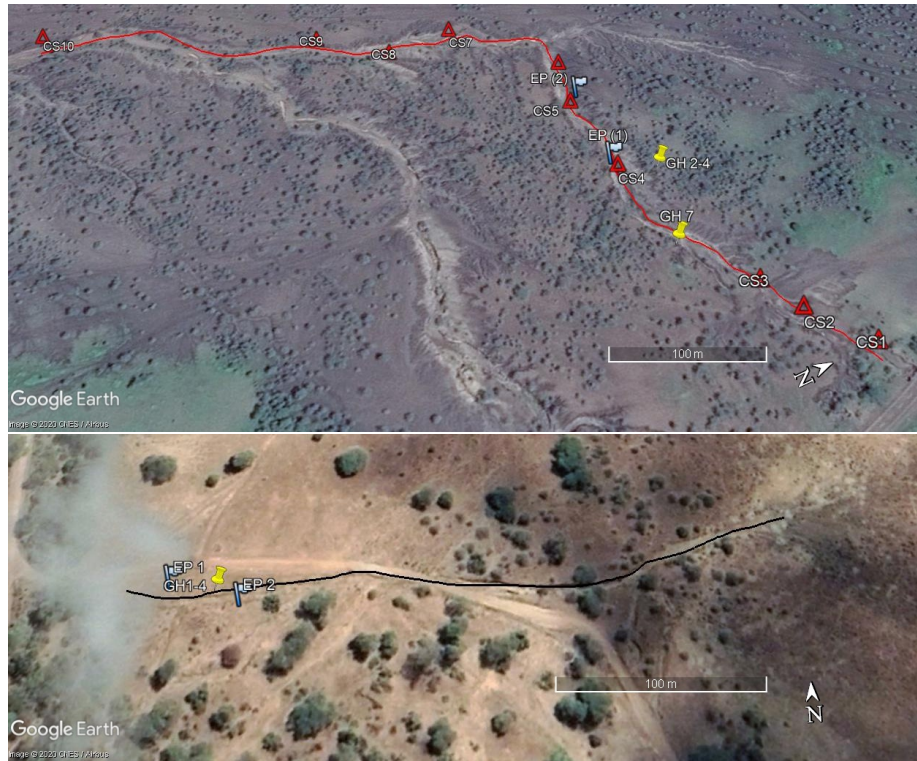


Figure 4: The locations of the various measuring points in GS1 and 2. EP refers to channel bed erosion pin and GH refers to gully head. In GS2 the cross-section measurements were taken at the EP1 and 2 location. The black and red line show the section of the gully system that was observed. Source: Google earth (2020)

The RS analysis provides a good indication of the magnitude of gully growth that can be found throughout the region. Six satellite images containing detailed pictures at different moments in time of gullies in the Lake Manyara watershed have been analyzed. The RS analysis also resulted in the identification of the two fieldwork areas GS1 and GS2 (figure 4). Most of these gully systems are in the northern and north-eastern parts of the Lake Manyara catchment. Table 4 shows the growth rates that were calculated using the RS images of the gullies at two different points in time.

Table 4. Results of the RS analysis showing the average monthly growth rate of six gullies, which was calculated by comparing the gully extent at two different points in time. <sup>1</sup>

| Gully head | Time (picture 1 – picture 2) | Average growth rate<br>(cm/month) |
|------------|------------------------------|-----------------------------------|
| RS GH 1    | 2/9/2017 – 9/23/2019         | 20                                |
| RS GH 2    | 2/9/2017 - 9/23/2019         | 18                                |
| RS GH 3    | 9/20/2014 – 3/13/2017        | 14                                |
| RS GH 4    | 1/14/2015 – 3/13/2017        | 11                                |
| RS GH 5    | 1/14/2015 – 3/13/2017        | 15                                |
| RS GH 6    | 1/14/2015 – 3/13/2017        | 38                                |

The growth rates were found to be varying between 11 to 38 cm month<sup>-1</sup> with an average value of 19.3 cm month<sup>-1</sup>. The six gullies that were studied in the RS analysis were chosen based on their similarities to the fieldwork gully systems GS1 and GS2. This is done because the RS analysis aims to compare the fieldwork measurements with other gully systems in the area. The RS gullies are all located on a terrain with a slope no exceeding 3%. The vegetation around the RS gullies is also like that of the fieldwork gullies, which means that some scattered Acacia trees are found around the gully systems. Furthermore, the RS gullies are in areas close to humans just as GS1.

### 3.3 Precipitation measurements

During the fieldwork period, precipitation measurements were also taken at two different locations (figure 5). It was assumed that precipitation data would best fit the erosion measurements if the measurement location of the precipitation is located near the fieldwork site, therefore two different precipitation datasets were used. For GS1 precipitation data were collected in the village of Mto Wa Mbu, which is 18km from GS1, and for GS2 the precipitation data were collected from a rain gauge at the gate of the National Park, located 9km from GS2. The precipitation data was used to analyze the relationship between erosion and precipitation.

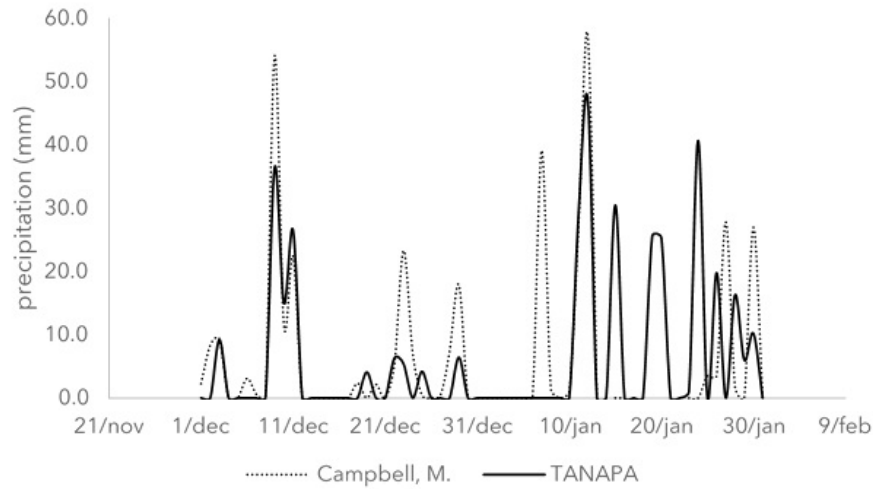


Figure 5: Two different sources of precipitation (mm) measurements from the fieldwork period. Source: TANAPA (2020), Campbell (2020).

### 3.4 Gully head monitoring

Over roughly two months measurements have been taken in GS1 and GS2. Tables 5 and 6 below show the measurements that were taken around six gully heads in GS1 and GS2. These measurements represent the growth of each gully head which is measured by measuring the distance between different fixed erosion pins and the gully head (figure 6). In some cases, the erosion pins had been fully removed which resulted in missing data at some dates. GS1 GH1 and GS1 GH5 were located at locations that made them prone to human-induced disturbance. On the 12<sup>th</sup> of December, all the erosion pins at GS1 GH1 and GS1 GH5 were removed after which these sites were abandoned. Also, on the 4<sup>th</sup> of January, all erosion pins were stolen at GS1 GH2, 3, and 4. These were replaced on the 11<sup>th</sup> of January. Eventually, 7 gully heads were used for further analysis (marked in bold in table 5 and 6).

Table 5. Erosion pin measurements (cm) representing the gully head growth of gully heads at a gully system (GS1). Only positions GH2, 3, and 4 have complete series due to the removal of pins at GH1 and GH5. Rem refers to removed followed by a “-” if the erosion pin has not yet been replaced.

| Date  | Rain | Gully head growth |      |      |      |      |      |      |      |      |      |      |      |      |      |      |      |      |      |      |      |      |      |
|-------|------|-------------------|------|------|------|------|------|------|------|------|------|------|------|------|------|------|------|------|------|------|------|------|------|
|       |      | GH1               |      |      | GH2  |      |      | GH3  |      |      | GH4  |      |      | GH5  |      |      | GH6  |      |      |      |      |      |      |
|       |      | Pin1              | Pin2 | Pin3 | Pin1 | Pin2 | Pin3 | Pin1 | Pin2 | Pin3 | Pin1 | Pin2 | Pin3 | Pin1 | Pin2 | Pin3 | Pin1 | Pin2 | Pin3 | Pin4 | Pin5 | Pin6 | Pin7 |
| dd-mm | mm   | cm                | cm   | cm   | cm   | cm   | cm   | cm   | cm   | cm   | cm   | cm   | cm   | cm   | cm   | cm   | cm   | cm   | cm   | Cm   | Cm   | cm   |      |
| 04-12 | 86.9 | 9                 | 13   | 5    | 3    | 6    | 2    | 0    | 32   | 4    | 3    | 19   | 1    | 0    | 41   | 4    |      |      |      |      |      |      |      |
| 18-12 | 2.3  | Rem               | Rem  | rem  | 4    | 2    | 1    | 0    | 3    | 1    | 8    | 1    | 4    | Rem  | Rem  | Rem  | 0    | 4    | rem  | rem  | 0    | 2    | 0    |
| 22-12 | 7.4  |                   |      |      | 1    | 11   | 2    | 2    | rem  | 5    | 2    | 11   | 2    |      |      |      | 0    | 1    | 9    | 5    | 0    | 1    | 7    |
| 26-12 | 30.7 |                   |      |      | rem  | 0    | 0    | 0    | -    | 4    | 4    | 0    | 0    |      |      |      | 0    | 0    | 3    | 2    | 2    | 0    | 0    |
| 29-12 | 25.7 |                   |      |      | 2    | 0    | 3    | 0    | -    | 8    |      | 8    | 3    |      |      |      | 5    | 1    | 0    | 1    | 1    | 3    | 2    |
| 04-01 | 0.0  |                   |      |      | rem  |      |      |      | 1    | 0    | 1    | 0    | 1    | 0    | 0    |
| 07-01 | 39.1 |                   |      |      | -    | -    | -    | -    | -    | -    | -    | -    | -    |      |      |      | 1    | 0    | 0    | Rem  | 0    | 4    | 0    |
| 11-01 | 29.4 |                   |      |      | -    | -    | -    | -    | -    | -    | -    | -    | -    |      |      |      | 0    | 0    | 0.5  | -    | 0    | 0    | 0    |
| 16-01 | 57.4 |                   |      |      | 5    | 11   | 0    | 0    | 7    | 0    | 3    | rem  | 3    |      |      |      | 0    | rem  | 0    | 12   | 0    | 0    | 0    |
| 27-01 | 34.8 |                   |      |      | 0    | 9    | 1    | 2    | 0    | 0    | 2    | -    | 5    |      |      |      | 4    | -    | 9    | 4    | 0    | 11   | 5    |

Table 6. Erosion pin measurements (cm) representing the gully head growth of a gully system (GS2) located in Lake Manyara National park, Tanzania.

| Date  | Rain | Gully head growth |      |      |      |
|-------|------|-------------------|------|------|------|
|       |      | GH1               | GH2  | GH3  | GH4  |
|       |      | Pin1              | Pin1 | Pin1 | Pin1 |
| dd-mm | mm   | cm                | cm   | cm   | cm   |
| 06-12 | 9.2  | 0.2               | 10.2 | 1    | 18   |
| 10-12 | 51.5 | 0                 | 0    | 1.5  | 0    |
| 13-12 | 26.5 | 0                 | 0    | 0    | 0    |
| 24-12 | 15.8 | 1                 | 0.2  | 1    | 0    |
| 27-12 | 4.2  | 0                 | 1    | 0    | 0    |
| 31-01 | 6.4  | 0                 | 0    | 0    | 0    |
| 08-01 | 0    | 2.5               | 0    | 4.5  | 0    |

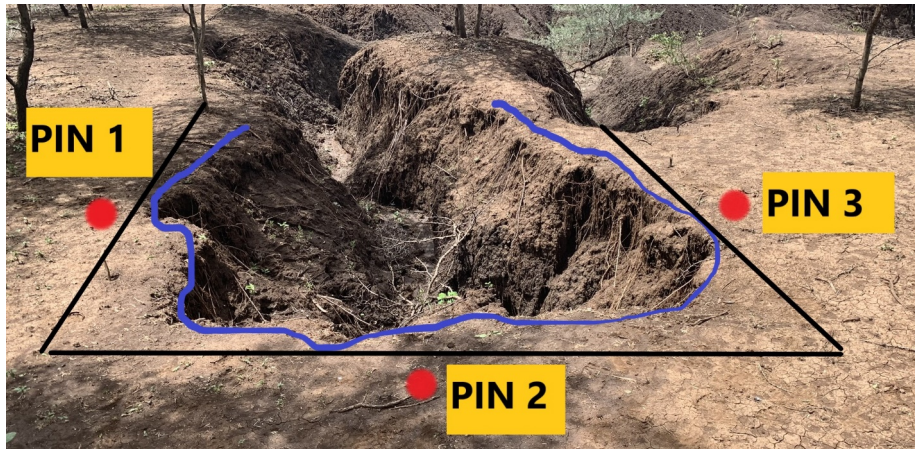


Figure 6: An example of three erosion pins around a gully head. Pin 1 and 3 measure the width increase of the gully head, pin 2 measures the lengthwise growth.

Based on the measurements that are shown in Tables 5 and 6 the growth rates of the different gully heads were calculated (Table 7). These growth rates were calculated by calculating the average measured erosion of each gully head. The average was used because not all measurement sites have an equal amount of erosion pins and using the sum of the measurements at each location will not correctly represent the growth rate. The growth rates shown in table 7 are lower than the growth rates from the RS analysis. The most likely explanation for this is that the RS analysis was performed over multiple years in most cases while the values in table 7 are based on just the short rainy season. The longer rain season occurs from March to May.

Table 7. The growth rates (cm/month) were calculated for each gully head and the average growth rate of each gully system (GS1 and GS2).<sup>2</sup>

| Gully head | Growth rate<br>(cm/month) | Average growth rate<br>(cm/month) |
|------------|---------------------------|-----------------------------------|
| GS1 GH2    | 11.7                      | 12.5                              |
| GS1 GH3    | 12.6                      |                                   |
| GS1 GH4    | 14.7                      |                                   |
| GS1 GH6    | 11.1                      |                                   |
| GS2 GH 1   | 3.3                       | 9.4                               |
| GS2 GH 2   | 10.5                      |                                   |
| GS2 GH 3   | 7.2                       |                                   |
| GS2 GH 4   | 16.5                      |                                   |

### 3.5 Channel bed erosion measurements

Besides monitoring the gully channels, channel bed erosion was also measured by measuring the height of various fixed erosion pins in the channel bed. An overview of the measurements that were taken at both locations can be found in tables 8 and 9. These values show that there are alternately events with erosion (positive values) and sedimentation (negative values). In Tables 8 and 9 there are multiple events where the erosion pins have been removed. The removal of erosion pins happened due to human and animal interaction. There is also an event where the erosion pin was washed away by excessive runoff. The erosion pin measurements of each measurement site in GS1 and GS2 have been summed up and an average was calculated to determine whether erosion or deposition occurred over the fieldwork period. It was found that GS1 has a net deposition (-2.3cm) while GS2 has a net erosion (0.47cm). This was calculated by summing up the average values for each measurement day. Because the channel bed erosion pins do not show an identifiable pattern or trend, the contribution of channel bed erosion to the total sediment mobilization in the gully system is uncertain.

Table 8. Channel bed erosion pin measurements (cm) which show the erosion and deposition in GS1. Negative values mean that the erosion pin decreased in size and thus represent deposition while positive values mean material was eroded around the erosion pin.

| Date  | Rain | Channel bed erosion |             |             |             |
|-------|------|---------------------|-------------|-------------|-------------|
|       |      | Site 1              |             | Site 2      |             |
| dd-mm | mm   | Pin 1<br>cm         | Pin 2<br>cm | Pin 3<br>cm | Pin 4<br>cm |
| 29-11 | 13.6 | -3                  | 1.5         | rem         | -4.2        |
| 16-12 | 91.7 | 0.5                 | 1.5         | 6           | 10          |
| 18-12 | 2.3  | -0.5                | 1.2         | 9.5         | -10.5       |
| 22-12 | 7.4  | 0                   | >1.2        | -2          | -2          |
| 26-12 | 30.7 | 0                   | rem         | 0           | -1.5        |
| 29-12 | 25.7 | 0                   | -           | 0           | 0.5         |
| 04-01 | 0.0  | 0.5                 | -           | 1           | -0.5        |
| 05-01 | 0.0  | 0                   | -           | 0           | 0           |
| 07-01 | 39.1 | -0.5                | 2           | -1          | 0           |
| 11-01 | 29.4 | 0.5                 | 2.5         | -0.5        | 0           |
| 16-01 | 57.4 | -4.3                | >2.5        | -1          | -0.5        |
| 27-01 | 34.8 | -1                  | rem         | 6           | 3.5         |

Table 9. Channel bed erosion pin measurements (cm) in Lake Man-yara national park (GS2). Negative values mean that the erosion pin decreased in size and thus represent deposition while positive values mean material was eroded around the erosion pin. Washed refers to an event where the flowing water within the gully channel washed away the erosion pin. Trampled refers to animal interaction.

| Date  | Rain | Channel bed erosion |             |             |             |             |
|-------|------|---------------------|-------------|-------------|-------------|-------------|
|       |      | Site 1              |             | Site 2      |             |             |
| dd-mm | mm   | Pin 1<br>cm         | Pin 2<br>cm | Pin 3<br>cm | Pin 4<br>cm | Pin 5<br>cm |
| 06-12 | 9.2  | 11.9                | washed      | 7.8         | 5.1         | 1.9         |
| 10-12 | 51.5 | -2                  | trampled    | -4          | -4.5        | -3.5        |
| 13-12 | 26.5 | -3                  | trampled    | -1.2        | 0.5         | 0.1         |
| 24-12 | 15.8 | -1.5                | -0.5        | 0.2         | 0           | -0.1        |
| 27-12 | 4.2  | -3.5                | 0           | -1.5        | -0.5        | -1          |
| 31-12 | 6.4  | 0                   | -1.5        | -1.5        | 2           | 1           |
| 03-01 | 0    | -0.5                | 1           | 0           | -1          | 0.5         |
| 08-01 | 0    | 0                   | -1          | 0           | 0.5         | trampled    |

### 3.6 Relation precipitation and gully erosion

The relation between the precipitation and the erosion data from both the channel bed and gully head erosion pins in GS1 and GS2 was further analyzed. No clear trend is visible in the graphs (figure 7), which was confirmed by statistical analyses. For only one of the eight gullies head a significant correlation with precipitation was found ( $p < 0.05$ ). The reason that except for one case no correlations exist is the locations of the precipitation measurement sites. For GS1 precipitation data were collected in the village of Mto Wa Mbu, which is 18km from GS1, and for GS2 the precipitation data were collected from a rain gauge at the gate of the National Park, located 9km from GS2. The distances between the rain gauges and the gullies were too large to detect any relation between rainfall gully growth.

The relation between precipitation and the erosion within the channel beds of GS1 and GS2 was also studied. Throughout the measurement period, there were alternating periods of deposition and erosion. Pearson correlations have been computed between the channel bed erosion pins and precipitation but did not yield any significant correlation ( $p < 0.05$ ). A *t*-test was used to analyze if there was a difference between the means of the channel bed erosion pin measurements in GS1 and GS2. But no significant difference in the mean values of the erosion pins in GS1 and GS2 was found ( $p < 0.05$ ). The same explanation as in the previous section can be given for the lack of correlation namely, the distance between the precipitation measurement locations and the fieldwork sites.

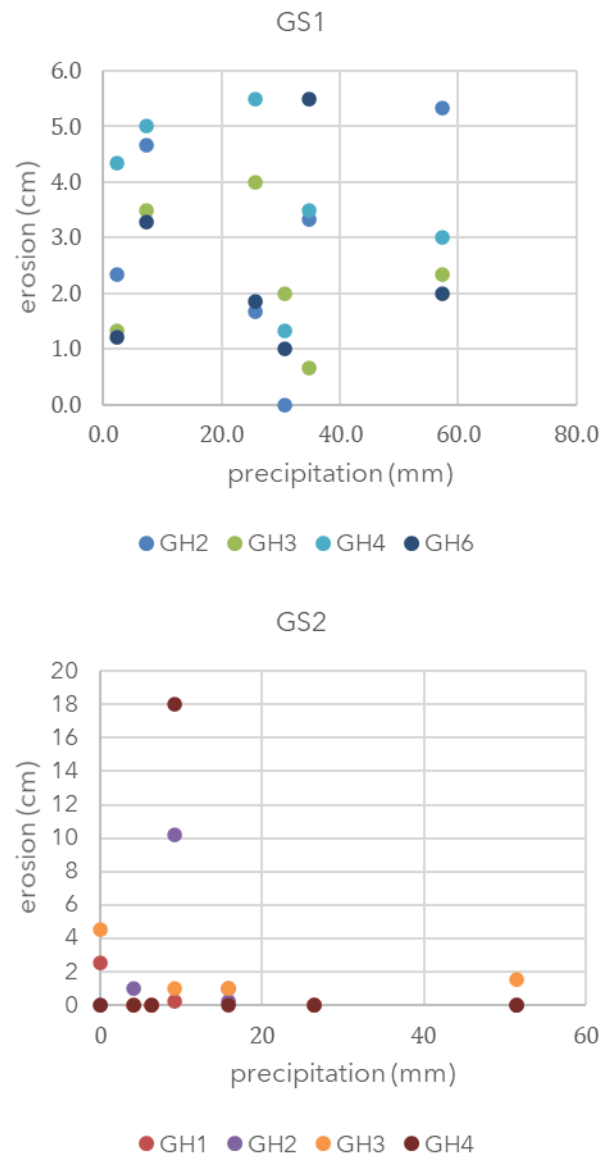


Figure 7: The relation between gully erosion rates and the amount of precipitation for gully systems GS1 (top) and GS2 (bottom)

### 3.7 Mobilized sediment in the gully systems

One of the main objectives is assessing the amount of sediment that is mo-

bilized and transported towards Lake Manyara. In this section, the amounts of mobilized sediment from the monitored gully heads and channel beds in GS1 and 2 are calculated (Table 10). The volume ( $\text{m}^3$ ) of eroded soil within the gully heads is determined by calculating the difference in volume between the gully head at the start and the end of the fieldwork period. The increase in width that was measured by the erosion pins and the increase in length is added to the initial values for the width and depth and in this way, the old and new volume can be compared. During the calculation of the volume, the gully is approximated as a rectangle (figure 6). The depth was only measured at one point in time and could not be repeated due to the removal of measuring equipment. The depth is therefore assumed to be constant in the volume calculation. The observations range from 0.47 to 1.71  $\text{m}^3$  per month in GS1 and from 0.01 to 0.06  $\text{m}^3$  for the studied gully heads in GS2. The amount of mobilized sediment is thus many times smaller inside the park, the dimensions of the gully head in GS2 are smaller and the lack of human disturbance is likely to decrease the amounts gully erosion.

. When comparing the precipitation that was measured during the fieldwork period with historical precipitation data, it shows that the rainfall in December (2019) and January (2020) is above average (TANAPA, 2020). The average rainfall in January and December is calculated with the help of a dataset from TANAPA (2020) which measured daily precipitation over 62 years. The average precipitation in January is 76.76 mm while the observed precipitation during the fieldwork period was 312.1mm, this is four times higher than the average (TANAPA, 2020). The average precipitation in December is 100.35mm while during the fieldwork period 113.6mm has been observed which is 1.13 times higher than average. It is expected that because of this above-average precipitation during the fieldwork period the observed erosion is also higher than average.

The average precipitation over the past decade is 621.16 mm per year (TANAPA, 2020) if we use this calculated decadal average precipitation, the estimated amount of eroded soil is between 0.78 and 2.85  $\text{m}^3$  in a year in GS1 and between 0.02 and 0.1  $\text{m}^3$  in GS2. It should however be noted that in this calculation a linear relationship is assumed between the gully erosion and precipitation but in reality, also other processes play a role such as the discussed animal and human interaction but also the intensity and frequency of the precipitation events.

Table 10. The volume of sediment that is produced by each gully head in GS1. This volume is calculated by calculating the difference between the gully volume at the start and end of the fieldwork period and then dividing it by the number of months to get the eroded volume per month.

| Gully head growth     |                       |                       |                       |                       |                       |                       |                       |
|-----------------------|-----------------------|-----------------------|-----------------------|-----------------------|-----------------------|-----------------------|-----------------------|
| GS1                   |                       |                       |                       | GS2                   |                       |                       |                       |
| GH2                   | GH3                   | GH4                   | GH6                   | GH1                   | GH2                   | GH3                   | GH4                   |
| m <sup>3</sup> /month |
| 0.47                  | 1.06                  | 0.671                 | 1.71                  | 0.01                  | 0.05                  | 0.02                  | 0.06                  |

### 3.8 Vegetation

In addition to gully head and channel monitoring, measurements have also been taken to construct cross sections in GS1 and GS2. With the help of these cross-sections, the effect of vegetation on the sidewall stability was studied. Because of the increased cohesion that is caused by the presence of vegetation, it was expected that the sidewall slopes of sidewalls with vegetation are steeper (figure 8). 11 cross-sections have been taken which are shown in figure 9. This analysis was only performed for the cross-sections that were taken in GS1 because, in GS2, not enough cross-sections were taken to do correct analysis. This analysis was done by determining the sidewall slope of all sidewalls in GS1 and subsequently dividing these sidewalls into two groups, one with and one without vegetation on the sidewall. Using the *t*-test ( $\alpha = 0.05$ ), no significant difference was found between the slopes with or without vegetation present on them. This is unexpected since previous studies indicated the strengthening effect of vegetation on soils which is why a higher sidewall slope was expected to be found on slopes with vegetation (Zhang et al., 2015).



Figure 8: The strengthening effect of vegetation on the soil can be seen in these images that were taken in GS1.

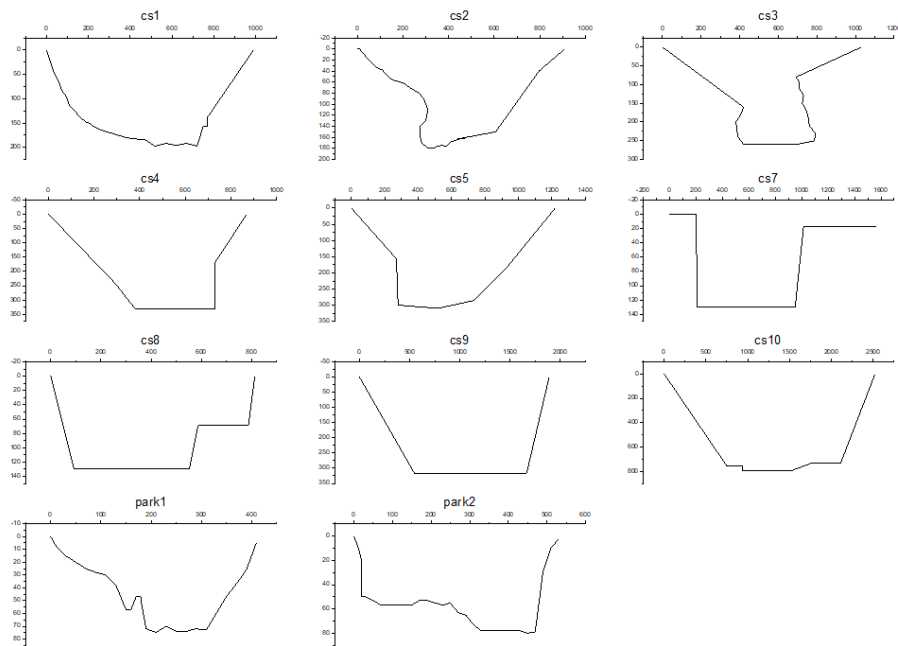


Figure 9: 11 different cross-sections that were taken in both GS1 (cs1-10) and GS2 (park1 and park 2).

### 3.9 Modeling of Land Use and Land Cover change

The modeling with SWAT was executed on the catchment of GS1 which has an area of 11.18 km<sup>2</sup> (figure 10). The north-eastern region of the sub-catchment contains steep elevation gradients while the rest of the area has little to no elevation gradients. The main types of landcover in the area are arid bush (RNGB) and grassland (RNGE) which cover 31% and 67% respectively (Table 11). Each landcover also has a unique CN value that SWAT uses to compute the surface runoff. The CN value is determined by SWAT based on the input data; no manual steps are needed in this process. Finally, the soils in the area are Andosols.

The main aim of the modeling is to quantify the amount of surface runoff and sediment that enter GS1 on average. This average is calculated over the entire modeling period which stretches over 35 years. Furthermore, the modeling assesses the effects of land-use change by increasing the agricultural land cover to 25% and studying the effects that this has on surface runoff (SURQ) and sediment yield (SYLD).

Table 11. The CN factor and area of the different land covers for the baseline scenario.

| Land cover                       | Area (km <sup>2</sup> ) | CN    |
|----------------------------------|-------------------------|-------|
| AGRL (agricultural land generic) | 0.04                    | 95.45 |
| RNGB (range-bush)                | 3.55                    | 85.10 |
| RNGE (range-grass)               | 7.59                    | 90.85 |

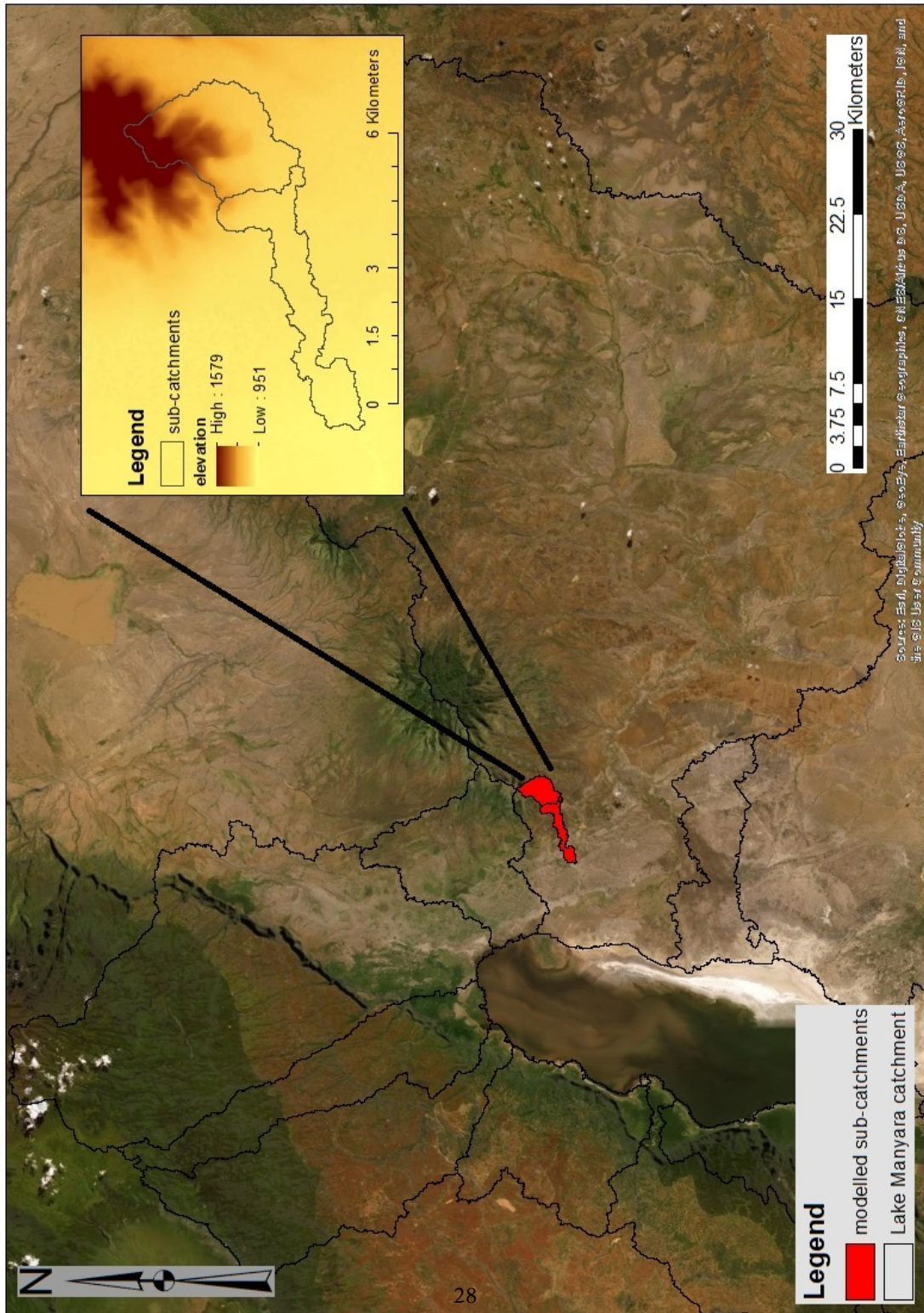


Figure 10: An overview of the location of the modeled area located in the Lake Manyara catchment. The smaller frame is zoomed in on the modeled catchment showing the elevation and HRUs.

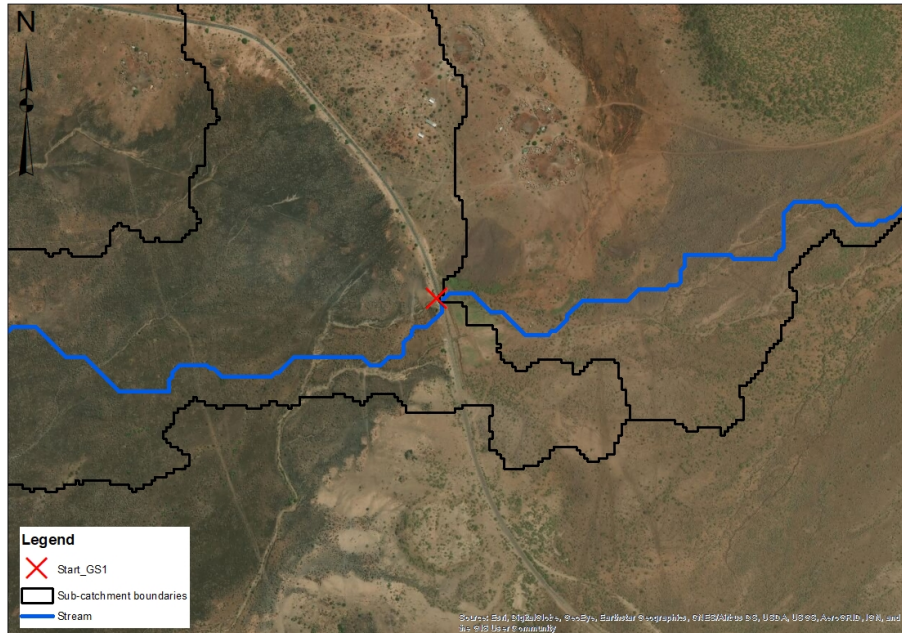


Figure 11: The borders of the two sub-catchments and in the middle, there is a marker that shows the exact location of the start of GS1.

SWAT was not able to correctly identify the gully system during the phase of stream network identification. This was caused by the spatial resolution of the DEM which was not high enough to recognize the gully system. The stream that is defined by SWAT does however correctly identify the start of GS1 (red cross in figure 11). Because of this, the area was divided into two sub-catchments. Sub-catchment 1 represents the area in which surface runoff is generated and sediment is mobilized which enters GS1. Even though sub-catchment 2 does not correctly represent the gully system it can still be used to gain insight into the dynamics of surface runoff and sediment mobilization. The CFSR (2020) daily weather data from 1979 until 2014 was used in the modeling. This weather data is essential for two reasons. First, the precipitation data is used by SWAT to determine surface runoff and erosion. Second, the weather data contains essential information on humidity, solar radiation, and other factors that drive the vegetation growth module. This vegetation growth module is important because this module allows for a realistic simulation of the study area in which there is a dynamic landcover throughout the year.

### 3.9.1 Current situation

Currently, the 15.7 and 4.5 t/ha/yr of sediment and 29.9 and 37.5 mm/yr of surface runoff are generated in sub-catchment 1 and 2, respectively (Table 12).

These values are the average yearly values which are calculated over the whole modeling period (1979-2014). Figure 12 visualizes both the SYLD and SURQ.

Table 12. The surface runoff (SURQ) and sediment yield (SYLD) in sub-catchment 1 and 2 for the current situation.

| Sub-catchment | SURQ (mm) | SYLD (t/ha) |
|---------------|-----------|-------------|
| 1             | 29.9      | 15.7        |
| 2             | 37.5      | 4.5         |

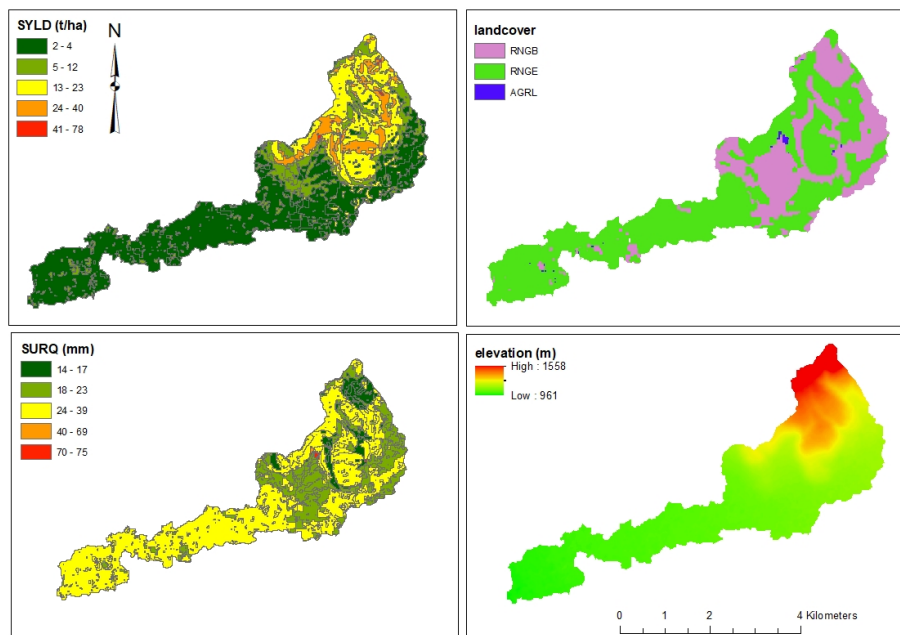


Figure 12: Top and bottom left show the sediment yield (SYLD) and surface runoff (SURQ) respectively. The top right and bottom right show the landcover and elevation profile of the modeled area.

The highest erosion values are exclusively found in the upper section of sub-catchment 1. This can be explained by the co-occurrence of RNGE – which has a higher CN value than RNGB – combined with steep elevation gradients. The SURQ shows a similar pattern in the upper regions. Here the high values of SURQ are found in the areas with co-occurrence of elevation gradients with RNGE. The steep elevation gradients increase the erosive potential. The lower section is where the SURQ and SYLD differ. The lower section of the study area has a relatively high SURQ which is again explained by the presence of mostly RNGE, there are a few isolated patches with a relatively low SURQ and in these locations the land cover is RNGB. It can be concluded that most runoff

is generated in the lower sections of the study area, the sediment on the other hand is produced in the upper regions where the elevation gradients increase the erosive potential of the flowing water.

GS1 has a definable link to Lake Manyara and it is therefore expected that part of the sediment that is generated in the modeled area is transported and deposited in Lake Manyara.

### 3.9.2 Precipitation, erosion, and runoff

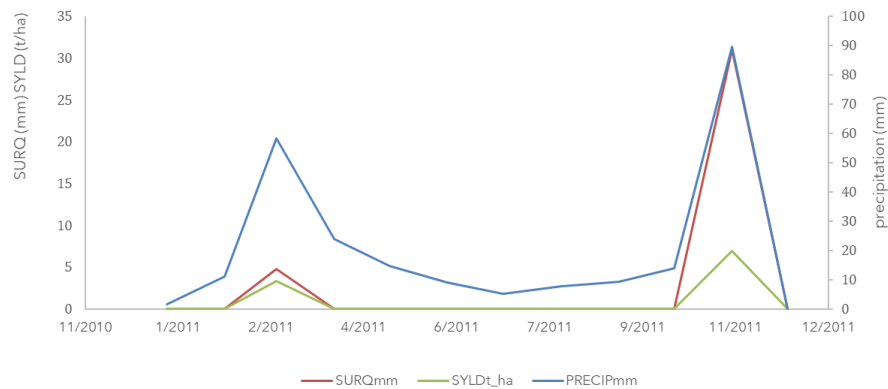


Figure 13: The relation between SURQ, SYLD, and precipitation in 2011 for the current situation.

Figure 13 shows that there is a clear relationship between the SURQ, SYLD, and precipitation. The year 2011 was chosen because the pattern and relation between the variables are pronounced in this year. The highest values for sediment yield and runoff occur around April and November, which are the yearly peaks in the two rainy seasons. So especially during this part of the year, the catchment is vulnerable to soil erosion. The two rain seasons that occur each year can thus be seen and accompany the highest values of soil erosion. There also seems to be a minimum threshold for the SURQ and SYLD to occur, this is visible in the figure between 4/2011 and 10/2011 because no SYLD and SURQ are generated in this period.

### 3.9.3 Increasing agricultural land cover

In line with the future predictions of a study by Wynants et al (2018), it is expected that natural land covers disappear and are replaced by agricultural land covers. Therefore, the scenario that was used in the modeling used this expected land cover change. The agricultural land cover in the modeled area was increased at the cost of RNGE, since this landcover is largest in the areas with little to no elevation gradients, and thus making it suitable for agriculture. Secondly, this landcover is most easily converted into agricultural land.

The increase in agricultural land that was modeled is 25%, so in total 25% of the study area will be covered with agricultural land. The values for SURQ and SYLD in table 13 show that both SURQ and SYLD increase when the agricultural land cover is increased. The SYLD increase of 34% and 78% is higher than that of the SURQ which is 13% and 18%. The overall increase of both SURQ and SYLD is explained by the fact that the CN value changes from 90.85 to 95.45 and thus significantly increasing the runoff potential. It is thus concluded that increasing the agricultural land cover increases both the SURQ and SYLD and is likely to enhance the gully erosion in this area.

Table 13. The surface runoff (SURQ) and sediment yield (SYLD) data for the current and future scenarios for sub-catchment 1 and 2.

| Sub-catchment | Current situation | Increased agriculture | % increase | Current situation | Increased agriculture | % increase |
|---------------|-------------------|-----------------------|------------|-------------------|-----------------------|------------|
|               | SURQ (mm)         | SURQ (mm)             |            | SYLD (t/ha)       | SYLD (t/ha)           |            |
| 1             | 29.9              | 34.0                  | 13         | 15.7              | 21.1                  | 34         |
| 2             | 37.5              | 44.2                  | 18         | 4.5               | 8.0                   | 78         |

### 3.10 Validation

As discussed earlier there is no data available that can be used for the calibration of the model, therefore the emphasis is on validating the modeling results. This validation was done by comparing the results that were produced by the model with results from similar studies in the same region (Karamage, 2018; Vanmaercke, 2014). A study by Vanmaercke (2014) is used to validate the calculated average yearly sediment yield values. Vanmaercke (2014) did an extensive literature study where he analyzed numerous studies that calculated sediment yields of different African catchments. From this study, 7 catchments were selected based on their location and size, and the sediment yield values from these catchments were used to validate the model results. A table containing sediment yield data from different Eastern African Countries can be found in Appendix A. Table 14, contains some summary statistics from the table in Appendix A.

Table 14. Summary statistics of the Sediment Yield (t/ha/yr) obtained from Vanmaercke (2014).

| Mean | Standard Error | Median | Standard deviation | Min  | Max   |
|------|----------------|--------|--------------------|------|-------|
| 9.9  | 3.7            | 7.0    | 9.8                | 1.56 | 31.32 |

15.7 and 4.5 t/ha/yr of sediment are generated in sub-catchment 1 and 2, respectively. This means that in sub-catchment 1 the sediment yield is 1.6 times higher than the average value that was calculated from the data of Vanmaercke (2014). In sub-catchments 2 the sediment yield is 2.2 times smaller. But as mentioned earlier, the modeled area was divided into two sub-catchments.

If we take the values from both sub-catchments and calculate an average, we find that the average sediment yield is 10.1, which is approximately equal to the mean of the study by Vanmaercke (2014). Another study that focused on measuring gully erosion in Kenya found similar values, in this study an average erosion of 11.19 t/ha/yr which is in line with the values of both Vanmaercke (2014) and the values found in the current study (Van Donger, 2015).

Karamage (2018) has focused on calculating the surface runoff by studying long-term monthly rainfall data from 1901 to 2017. In Appendix B a figure can be found showing the surface runoff in Africa for each month as well as annual values for the surface runoff. From the figure in Appendix B, it can be concluded that all surface runoff values are between 0 and 50 mm in all months. From this research, it can be concluded that the 33.3mm of runoff that is calculated by SWAT for the current situation, can be validated with the help of the study by Karamage (2018). Another study that was executed in Tanzania

Based on these findings it can be concluded that surface runoff and sediment yield that was calculated by SWAT can be validated and backed by other studies.

## 4 Discussion and Conclusion

Fieldwork measurements were taken over roughly two months. These fieldwork measurements found similar values in both the RS analysis and the fieldwork. The RS analysis showed average growth rates ranging from 11-38 cm/month which are in the same order of magnitude as the 12.5 and 9.4 cm/month that were found in GS1 and GS2, respectively. The growth measurements were used to derive the amount of eroded soil, which was found to be between 0.47 to 1.71 m<sup>3</sup> per month in GS1 and from 0.01 to 0.06 m<sup>3</sup> in GS2.

The precipitation during the measurement period was higher than on average, if taking into consideration the average precipitation over the past decade then the yearly gully head sediment mobilization is expected to be between 0.78 m<sup>3</sup> and 2.85 m<sup>3</sup> per year and 0.02 and 0.1 m<sup>3</sup> per year for GS1 and GS2 respectively. It should however be noted that in this calculation a linear relationship is assumed between the gully erosion and precipitation. The gully erosion that was measured in GS2 is lower than that in GS1. The dimensions found in GS1 are many times larger than those of GS2, which also explains the difference in gully erosion. But more interesting is the question, why no gullies with the dimensions as found in GS1 are present inside the park. An explanation is that the absence of human disturbances and because of this a large diversity of flora and fauna increases the resistance of this area to soil erosion.

The erosion pin measurements have not been able to establish a clear link between precipitation and erosion. The rainfall data does not seem to be accurately representing the local precipitation at the measurement sites, making it difficult to correlate the two variables. Gully erosion is not a constant linear

process. The gullies grow, in most cases, by slope failure where a large part of a gully head or sidewall collapses thus resulting in times of rapid gully growth by sidewall failures followed by periods of relatively little activity. The gully system in Lake Manyara (GS2) seemed to have little to no gully erosion and the gully erosion that was present had values that were incomparable to the dimensions found in GS1. This is most likely caused by the fact that no people live in this area and because of this no big herds of livestock roam and graze this area. The vegetation is also more diverse in and around GS2 which is a likely explanation for the absence of severe gully erosion. This is possibly also explained by the lack of human interaction with nature in this area. On the eastern side of the lake – GS1 is located on this side – many gullies can be seen while driving through the area. In the Lake Manyara national park, on the other hand, only one gully system could be found, which strengthens the idea that the lack of human interference is what causes little gully erosion to be present.

Further, SWAT has been used to gain insight into the dynamics and quantities of surface runoff and sediment mobilization in two small sub-catchments in the Lake Manyara catchments. SWAT found that currently between 29.9 and 37.5mm of surface runoff is generated on average in the modeled area. Also, the sediment yield was computed, and SWAT calculated that between 15.7 and 4.5 t/ha/yr of sediment produced yearly. Based on the predictions of a study by Wynants et al. (2019) agricultural landcover is likely to expand at the cost of natural vegetation. This scenario has been modeled with SWAT and the results show that increasing the agricultural land cover also increases the surface runoff and sediment yield in the modeled area. In other words, increasing agriculture also causes increased soil erosion. As with all models, SWAT creates a simplification of reality, and it is thus just an approximation of reality. In the case of the current study, no verified field data could be used as model input. The soil map consisted of only one soil type; the precipitation data was measured on a location outside of the modeled area which is also not optimal. Moreover, the DEM with a resolution of 12.5x12.5 meters for a small catchment is not ideal. Nevertheless, this was the best available data. The model results could be verified by other studies and more importantly, gave valuable insight into the potential effect of land-use change. Even though the model does not specifically model gully erosion, the results still provides a good starting point for future research to find out how much of the mobilized sediment actually comes from gully erosion. The data also shows what areas are prone to soil erosion and pinpoints areas of increased gully formation and erosion risk. Based on various studies the measured soil erosion is above average compared to other studies. Fenta et al. (2020) concluded from their research that the national average soil loss in Tanzania is 4.1 t/ha/yr, the maximum of 15.7 t/ha/yr that was found in the current study is almost 4 times as high. In short, the current measured and modeled erosion is relatively high, and based on the modeling it is expected that if the trend of increased agriculture continues the already high amounts of sediment mobilization will further increase. Causing loss of valuable soil in the area.

At this time there is too much uncertainty and too little data to judge how much sediment is delivered to Lake Manyara by gully erosion. More field data is needed. This study only focused on channel bed and gully head erosion while also other processes produce sediment such as gully channel sidewall collapse. Furthermore, gully erosion is only studied in two relatively small gully systems which makes it hard to generalize the results since little is known about gully erosion in the rest of the catchment. Moreover, data is missing on how much sediment is transported to Lake Manyara. Overall, precipitation is expected to decrease in the Lake Manyara catchment (Keijzer, 2020). And a decrease in precipitation will - in the short term - cause a decrease in surface runoff and erosion. However, draughts also harm the vegetation in the area which could cause the resistance to erosion to decrease which in turn would lower the threshold for soil erosion. This is also an interesting and important topic for future research to focus on. It is however certain that gully erosion is very active in the catchment and that high amounts of gully erosion were measured during the fieldwork period.

In conclusion, high amounts of erosion were measured in the Lake Manyara catchment. This study also showed that an expected increase in agricultural land cover will likely increase the erosion in this area. Even though too little data is present to make statements about the role of gully erosion in sediment delivery to Lake Manyara it can be concluded that gully erosion is an active process in the studied areas.

## 5 References

- African Wildlife Foundation. (2003). *Lake Manyara Watershed Assessment. Lake Manyara Watershed Assessment*. (Progress report)
- Alaska Satellite Facility (ASF). ASF DAAC 2015; Includes JAXA/METI 2007. Available at: <http://dx.doi.org/10.5067/Z97HFCNKR6VA> [Accessed on 14 Apr. 2020].
- Bachofer, F., Quénéhervé, G., & Märker, M. (2014). The Delineation of Paleo-Shorelines in the Lake Manyara Basin Using TerraSAR-X Data. *Remote Sensing*, 6(??), 2195–2212. doi: 10.3390/rs6032195
- Bagarello, V. and Sgroi, A. (2004). Using the single-ring infiltrometer method to detect temporal changes in surface soil field-saturated hydraulic conductivity. *Soil and Tillage Research*, 76(??), pp.13- 24.
- Bashir, S., Javed, A., Bibi, I. and Ahmad, N. (2017). Soil and Water Conservation. [online] Available at: <https://www.researchgate.net/publication/320729156> [Accessed 6 Sep. 2019].
- Blake, W. H., Rabinovich, A., Wynants, M., Kelly, C., Nasser, M., Ngondya, I., ... Ndakidemi, P. (2018). Soil erosion in East Africa: an interdisciplinary approach to realizing pastoral land management change. *Environmental Research Letters*, 13(??), 124014. doi: 10.1088/1748-9326/aaea8b
- Borrelli, P., Robinson, D. A., Fleischer, L. R., Lugato, E., Ballabio, C., Alewell, C., ... Panagos, P. (2013). An assessment of the global impact of 21st-century land-use change on soil erosion. *Nature Communications*, 8. doi: 10.1038/s41467-017-02142-7
- Capra, A. (2013). Ephemeral gully and gully erosion in cultivated land: a review. In: *Dprecipitationage Basins and Catchment Management*. [online] Nova Science Publishers, pp.110-134. Available at: [https://www.researchgate.net/publication/261322489\\_Ephemeral\\_gully\\_and\\_gully\\_erosion\\_in\\_cultivated\\_land\\_A\\_review](https://www.researchgate.net/publication/261322489_Ephemeral_gully_and_gully_erosion_in_cultivated_land_A_review) [Accessed 6 Sep. 2019].
- CFSR: Global Weather Data for SWA (n.d.). Retrieved April 8, 2020, from <https://globalweather.tamu.edu/>
- Chen, J., Xiao, H., Li, Z., Liu, C., Wang, D., Wang, L., & Tang, C. (2019). Threshold effects of vegetation coverage on soil erosion control in small watersheds of the red soil hilly region in China. *Ecological Engineering*, 132, 109–114. doi: 10.1016/j.ecoleng.2019.04.010

Deus, D., & Gloaguen, R. (2013). Remote Sensing Analysis of Lake Dynamics in Semi-Arid Regions: Implication for Water Resource Management. Lake Manyara, East African Rift, Northern Tanzania. *Water*, 5(??), 698–727. doi: 10.3390/w5020698

Deus, D., Gloaguen, R., & Krause, P. (2013). Water Balance Modeling in a Semi-Arid Environment with Limited in situ Data Using Remote Sensing in Lake Manyara, East African Rift, Tanzania. *Remote Sensing*, 5(??), 1651–1680. doi: 10.3390/rs5041651

Durán Zuazo, V. and Rodríguez Pleguezuelo, C. (2008). Soil erosion and runoff prevention by plant covers. A review. *Agronomy for Sustainable Development*, 28(??), pp.65-86.

FAO. (1991). Food and Agriculture Organization of the United Nations. Retrieved March 17, 2020, from <http://www.fao.org/>

Feng, Y., Mu, H., Qin, F., Deng, Q., Liu, H., Zhang, B., Luo, M., Liu, S. and Liu, G. (2017). Modeling the morphology of gully cross sections in the Yuanmou Dry-hot Valley. *Physical Geography*, 38(??), pp.448-469.

Fenta, A. A., Tsunekawa, A., Haregeweyn, N., Poesen, J., Tsubo, M., Borrelli, P., . . . Kurosaki, Y. (2020). Land susceptibility to water and wind erosion risks in the East Africa region. *Science of The Total Environment*, 703, 135016. doi:10.1016/j.scitotenv.2019.135016

Flores-Cervantes, J., Istanbuloglu, E., & Bras, R. (2006). Development of gullies on the landscape: A model of headcut retreat resulting from plunge pool erosion. *Journal Of Geophysical Research*, 111(F1). doi: 10.1029/2004jf000226

Ghimire, S., Higaki, D. and Bhattarai, T. (2013). Estimation of Soil Erosion Rates and Eroded Sediment in a Degraded Catchment of the Siwalik Hills, Nepal. *Land*, 2(??), pp.370-391.

Githui, F., Mutua, F., & Bauwens, W. (2009). Estimating the impacts of land-cover change on runoff using the soil and water assessment tool (SWAT): case study of Nzoia catchment, Kenya / Estimation des impacts du changement d'occupation du sol sur l'écoulement à l'aide de SWAT: étude du cas du bassin de Nzoia, Kenya. *Hydrological Sciences Journal*, 54(??), 899–908. doi: 10.1623/hysj.54.5.899

Hessel, R., & van Asch, T. (2003). Modeling gully erosion for a small catchment on the Chinese Loess Plateau. *CATENA*, 54(1-2), 131-146. doi: 10.1016/s0341-8162(??)00061-4

Homewood, K. M., Trench, P. C., & Brockington, D. (2012). Pastoralist livelihoods and wildlife revenues in East Africa: a case for coexistence? *Pastoralism*:

*Research, Policy and Practice*, 2(??). doi: 10.1186/2041-7136-2-19

Homewood, K., Kristjanson, P. and Trench, P. (2009). Changing land use, livelihoods, and wildlife conservation in Maasailand. In: *Staying Maasai? Livelihoods, Conservation and Development in East African Rangelands*. New York: Springer.

Hoogenboom, P. (2013). Sediment yield by gully erosion in a sub catchment of the Awassa watershed, Ethiopia. (MSc Thesis). Utrecht University, Utrecht, The Netherlands.

Istanbulluoglu, E., Bras, R., Flores-Cervantes, H. and Tucker, G. (2005). Implications of bank failures and fluvial erosion for gully development: Field observations and modeling. *Journal of Geophysical Research*, 110. doi: 10.1029/2004JF000145

Karamage, F., Liu, Y., Fan, X., Justine, M. F., Wu, G., Liu, Y., ... Wang, R. (2018). Spatial Relationship between Precipitation and Runoff in Africa. *Hydrology and Earth System Sciences Discussions*, 1–27. doi: 10.5194/hess-2018-424

Keijzer, T. (2020) *Drought analysis of the Lake Manyara catchment* (MSc Thesis). Utrecht University, Utrecht, the Netherlands.

Kirkby, M. and Bracken, L. (2009). Gully processes and gully dynamics. *Earth Surface Processes and Landforms*, 34(??), pp.1841-1851.

Kiunsi, R. and Meadows, M. (2006). Assessing land degradation in the Monduli District, northern Tanzania. *Land Degradation & Development*, 17(??), pp.509-525.

Leopold, L.B., Wolman, M.G., Miller, J.P. (1964). *Fluvial processes in geomorphology*. Freeman, San Francisco.

Maerker, M., Quénéhervé, G., Bachofer, F., & Mori, S. (2015). A simple DEM assessment procedure for gully system analysis in the Lake Manyara area, northern Tanzania. *Natural Hazards*, 79(S1), 235– 253. doi: 10.1007/s11069-015-1855-y

Maitima, j m, Mugatha, S. M., Reid, R. S., Gachimbi, L. N., Majule, A., Lyaruu, H., ... Mugisha, S. (2009). The linkages between land-use change, land degradation and biodiversity across East Africa. *African Journal of Environmental Science and Technology*, 3(??), 310–325. Retrieved from [https://www.researchgate.net/publication/228913785\\_The\\_linkages\\_between\\_land\\_use\\_change\\_land\\_degradation\\_and\\_biodiversity\\_across\\_East\\_Africa](https://www.researchgate.net/publication/228913785_The_linkages_between_land_use_change_land_degradation_and_biodiversity_across_East_Africa)

Martinez-Casasnovas, J.A., Ramos, M., & Poesen, J. (2004). Assessment of side-wall erosion in large gullies using multi-temporal DEMs and logistic regression analysis. *Geomorphology*, 58(1-4), 305–321. doi: 10.1016/j.geomorph.2003.08.005

Montanarella, L., Pennock, D. J., McKenzie, N., Badraoui, M., Chude, V., Baptista, ... Vargas, R. (2016). World's soils are under threat, *SOIL*, 2, 79-82. <https://doi.org/10.5194/soil-2-79-2016>

Mosbahi, M., Benabdallah, S. and Boussema, M. (2012). Assessment of soil erosion risk using SWAT model. *Arabian Journal of Geosciences*, 6(??), pp.4011-4019.

National Bureau of Statistics (2013). *2012 population and housing census*. Dar es Salaam: National Bureau of Statistics, Ministry of Finance.

Nazari-Sharabian, M., Karakouzian, M., & Ahmad, S. (2019). Effect of DEM Resolution on Runoff Yield, and Sensitivity of Parameters Contributing to Runoff in a Watershed. doi: 10.20944/preprints201901.0192.v1

NCAR. (2019). Climate Forecast System Reanalysis (CFSR). Retrieved April 29, 2020, from <https://climatedataguide.ucar.edu/climate-data/climate-forecast-system-reanalysis-cfsr>

Neitsch, S.L., Arnold, J.G., Kiniry, J.R. and Williams, J.R., 2011. *Soil and Water Assessment Tool Theoretical Documentation Version 2009*. College Station: Texas Water Resources Institute. Available at: <http://swat.tamu.edu/media/99192/swat2009-theory.pdf> [Accessed 14 Apr. 2020].

Nkonya, E., Anderson, W., Kato, E., Koo, J., Mirzabaev, A., Braun, J. V., & Meyer, S. (2015). Global Cost of Land Degradation. *Economics of Land Degradation and Improvement – A Global Assessment for Sustainable Development*, 117–165. doi: 10.1007/978-3-319-19168-3\_6

Oostwoud Wijdenes, D., Poesen, J., Vandekerckhove, L. and Ghesquiere, M. (2000). Spatial distribution of gully head activity and sediment supply along an ephemeral channel in a Mediterranean environment. *CATENA*, 39(??), pp.147-167.

Pimentel, D., Harvey, C., Resosudarmo, P., Sinclair, K., Kurz, D., Mcnair, M., ... Blair, R. (1995). Environmental and Economic Costs of Soil Erosion and Conservation Benefits. *Science*, 267(5201), 1117–1123. doi: 10.1126/science.267.5201.1117

QIU, L., ZHENG, F., & YIN, R. (2012). SWAT-based runoff and sediment simulation in a small watershed, the loessial hilly-gullied region of China: capabili-

- ties and challenges. *International Journal Of Sediment Research*, 27(??), 226-234. doi: 10.1016/s1001-6279(??)60030-4
- Schoorl, J., Veldkamp, A. and Bouma, J. (2002). Modeling Water and Soil Redistribution in a Dynamic Landscape Context. *Soil Science Society of America Journal*, 66(??), p.1610.
- Sidorchuk, A. (2006). Stages in gully evolution and self-organized criticality. *Earth Surface Processes and Landforms*, 31(??), pp.1329-1344.
- Stolte, J., Liu, B., Ritsema, C., van den Elsen, H., & Hessel, R. (2003). Modeling water flow and sediment processes in a small gully system on the Loess Plateau in China. *CATENA*, 54(1-2), 117-130. doi: 10.1016/s0341- 8162(??)00060-2
- SWAT (n.d.). ArcSWAT. [online] Swat.tamu.edu Available at: <https://swat.tamu.edu/software/arcswat/> [Accessed 29 Oct. 2019].
- TANAPA (2020) rainfall data April 1954 to 2020 [spreadsheet]. Lake Manyara National Park, TANAPA.
- UNDA (n.d.). *Brackishwater aquaculture development and precipitation project* (Annex 1). Manila, Philippines: UNDP.
- USDA. (n.d.). *Ephemeral Gully Erosion— A National Resource Concern. Ephemeral Gully Erosion— A National Resource Concern* (Report No.69). USDA.
- Van der Hoeven, S. (2016). Soil erosion modeling using LISEM in agricultural fields at the foot of the Sierras Chicas, Córdoba, Argentina. (MSc Thesis). Wageningen University, Wageningen, The Netherlands.
- Van Dijk, M. (2016). *Modeling the hydrology in the Lake Awassa catchment, Ethiopia* (MSc Thesis). Utrecht University, Utrecht, The Netherlands.
- Van Dongen, R. (2015). *Modeling soil redistribution and gully head retreat; analyzing the effect of climate and land management*. Master Thesis. Wageningen University.
- Van Mens, L. (2016). *Unravelling the hydrological dynamics of Lake Manyara in Tanzania* (MSc Thesis). Utrecht University, Utrecht, the Netherlands.
- Vanacker, V., von Blanckenburg, F., Govers, G., Molina, A., Poesen, J., Deckers, J., & Kubik, P. (2007). Restoring dense vegetation can slow mountain erosion to near natural benchmark levels. *Geology*, 35(??), 303. doi: 10.1130/g23109a.1

Vanmaercke, M., Poesen, J., Broeckx, J., & Nyssen, J. (2014). Sediment yield in Africa. *Earth-Science Reviews*, 136, 350–368. doi: 10.1016/j.earscirev.2014.06.004

Verhoeve, S. (2019). *Satellite based analysis of environmental changes in the Monduli and Longido districts, Tanzania* (MSc Thesis). Utrecht University, Utrecht, the Netherlands.

Wilson, G. V., Nieber, J. L., Sidle, R. C., & Fox, G. A. (2013). Internal Erosion during Soil Pipeflow: State of the Science for Experimental and Numerical Analysis. *Transactions of the ASABE*, 56(??), 465–478. doi: 10.13031/2013.42667

Wu, Y., Zheng, Q., Zhang, Y., Liu, B., Cheng, H., & Wang, Y. (2008). Development of gullies and sediment production in the black soil region of northeastern China. *Geomorphology*, 101(??), 683–691. doi: 10.1016/j.geomorph.2008.03.008

Wynants, M. (2018). Pinpointing areas of increased surface erosion following land cover changes using RUSLE modeling and sediment fingerprinting: A case study of the Lake Manyara catchment, Tanzania. doi: 10.13140/RG.2.2.27177.95846.

Wynants, M. (2019). Assessing the dynamics of soil erosion and sediment transport under increasing land use pressures in east-African rift catchments (Unpublished doctoral dissertation). University of Plymouth, Plymouth.

Wynants, M., Kelly, C., Mtei, K., Munishi, L., Patrick, A., Rabinovich, A., ... Ndakidemi, P. (2019). Drivers of increased soil erosion in East Africa's agro-pastoral systems: changing interactions between the social, economic and natural domains. *Regional Environmental Change*. doi: 10.1007/s10113-019-01520-9

Wynants, M., Millward, G., Patrick, A., Taylor, A., Munishi, L., Mtei, K., ... Blake, W. (2020). Determining tributary sources of increased sedimentation in East-African Rift Lakes using a combination of sediment tracing and radioactive dating. *Science of the Total Environment*, 717. doi: 10.5194/egusphere-egu2020-10686

Wynants, M., Solomon, H., Ndakidemi, P., & Blake, W. H. (2018). Pinpointing areas of increased soil erosion risk following land cover change in the Lake Manyara catchment, Tanzania. *International Journal of Applied Earth Observation and Geoinformation*, 71, 1–8. doi: 10.1016/j.jag.2018.05.008

Xu, M., Dong, X., Yang, X., Chen, X., Zhang, Q., Liu, Q., Wang, R., Yao, M., Davidson, T. and Jeppesen, E. (2017). Recent Sedimentation Rates of Shallow

Lakes in the Middle and Lower Reaches of the Yangtze River: Patterns, Controlling Factors and Implications for Lake Management. *Water*, 9(??), p.617.

Zegeye, A., Langendoen, E., Stoof, C., Tilahun, S., Dagneu, D., Zimale, F., Guzman, C., Yitaferu, B. and Steenhuis, T. (2016). Morphological dynamics of gully systems in the sub-humid Ethiopian Highlands: The Debre Mawi watershed. *SOIL Discussions*, pp.1-29.

Zhang, L., Wang, J., Bai, Z. and Lv, C. (2015). Effects of vegetation on runoff and soil erosion on reclaimed land in an opencast coal-mine dump in a loess area. *CATENA*, 128, pp.44-5

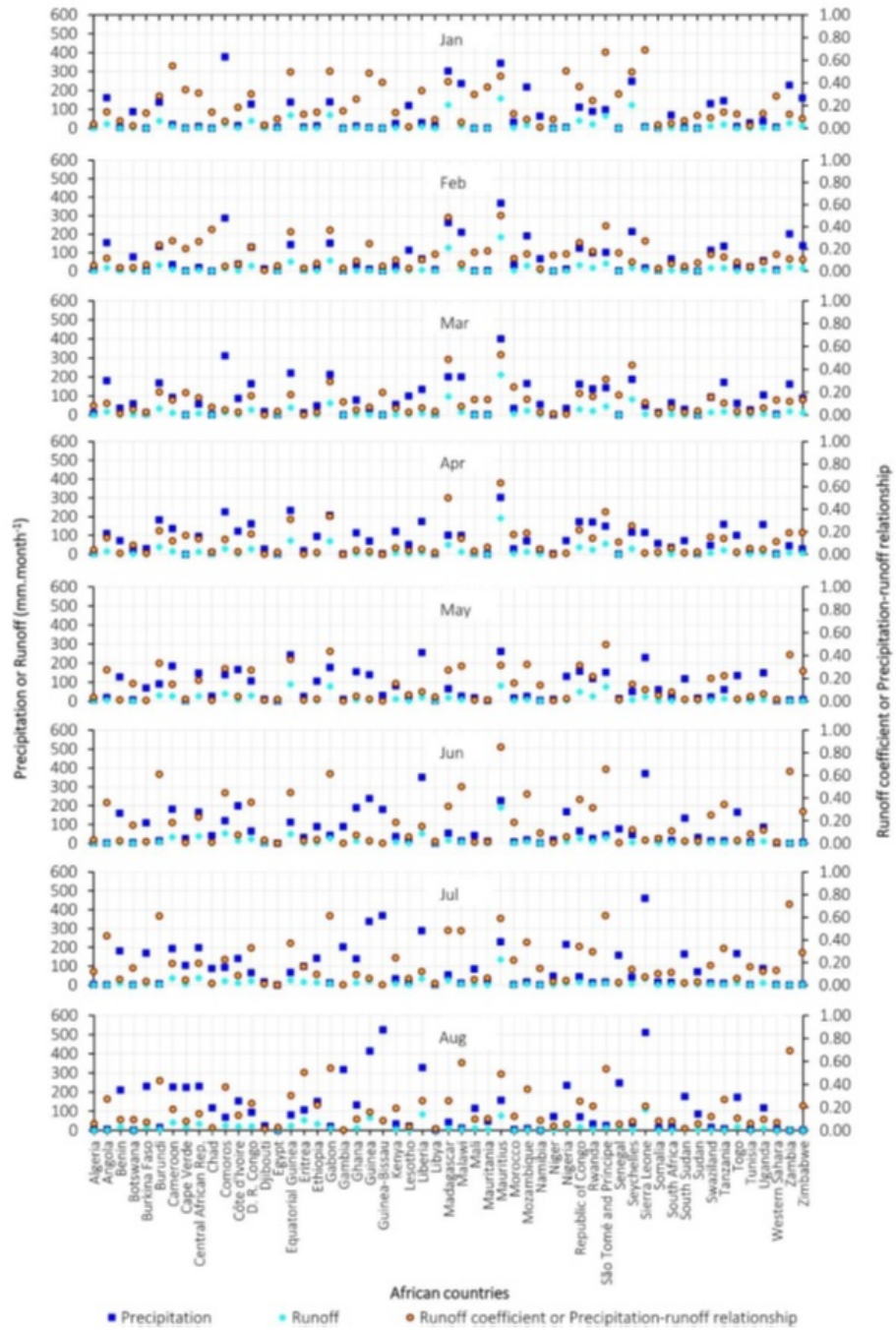
## 6 Appendix

### 6.1 Appendix A

Table 15. Sediment yields (t/km<sup>2</sup>/y) in different catchments in several East African Countries. This table has been retrieved and adapted from Vanmaercke (2014).

| Country  | measuring location        | Lat (°) | Lon (°) | Area (km <sup>2</sup> ) | SY (t/ha/y) | Measuring Period    | Measuring Period | Reference                      |
|----------|---------------------------|---------|---------|-------------------------|-------------|---------------------|------------------|--------------------------------|
| Tanzania | <u>Igurubi</u>            | -3.9993 | 33.7066 | 1.2                     | 10.78       | 1959 - 1978         | 19               | <u>Ndomba, 2011</u>            |
| Tanzania | <u>Imagi</u>              | -6.2061 | 35.7552 | 1.5                     | 7.01        | 1930 - 1971         | 42               | Rapp et al., 1972              |
| Tanzania | <u>Mbola</u>              | -4.8776 | 32.7211 | 6.4                     | 6.34        | 1972 - 1978         | 6                | <u>Ndomba, 2011</u>            |
| Tanzania | Outlet in lake Tanganyika | -4.626  | 29.642  | 7                       | 31.32       | Nov 1997 - Oct 1998 | 1                | <u>Nkotagu en Mbwano, 2000</u> |
| Tanzania | <u>Ulaya</u>              | -4.3992 | 33.4503 | 8.3                     | 1.56        | 1947 - 1978         | 31               | <u>Ndomba, 2011</u>            |
| Tanzania | <u>Msalatu</u>            | -6.2038 | 35.772  | 8.7                     | 5.03        | 1944 - 1971         | 28               | Rapp et al., 1972              |
| Tanzania | <u>Kisongo</u>            | -3.3391 | 36.5778 | 9.3                     | 7.37        | 1960 - 1971         | 12               | Rapp et al., 1972              |

## 6.2 Appendix B



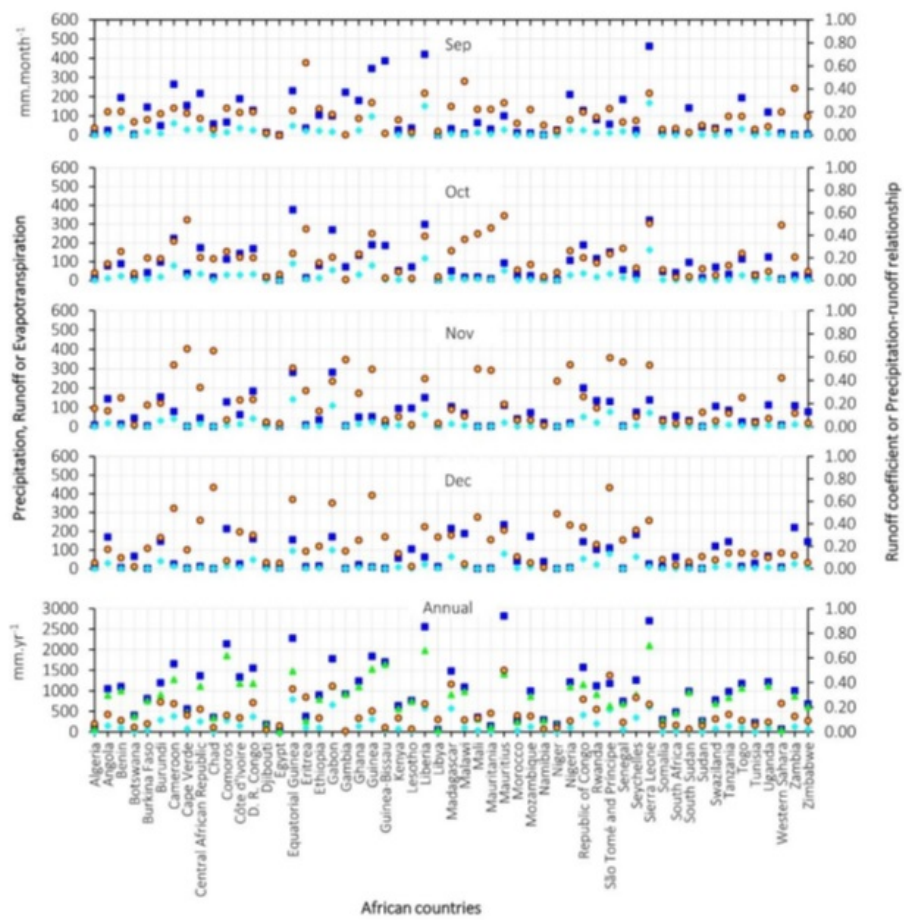


Figure 14: The relation between SURQ, SYLD, and precipitation in 2011 for the current situation.